

AMERICAN UNIVERSITY OF BEIRUT

CHARACTERIZATION OF POST-TRAUMATIC EPILEPTIFORM
FEATURES AND BEHAVIORAL DISTURBANCES IN A
CLINICALLY-RELEVANT RODENT MODEL OF
HEMORRHAGIC CLOSED-HEAD INJURY

by
DOUNYA FOUAD JALLOUL

A thesis
submitted in partial fulfillment of the requirements
for the degree of Master of Science
to the Interfaculty Graduate Program of Neuroscience
Department of Anatomy, Cell Biology and Physiological Sciences
of the Faculty of Medicine at the American University of Beirut

Beirut, Lebanon
September 2019

AMERICAN UNIVERSITY OF BEIRUT

CHARACTERIZATION OF POST-TRAUMATIC EPILEPTIFORM FEATURES
AND BEHAVIORAL DISTURBANCES IN A CLINICALLY RELEVANT RODENT
MODEL OF HEMORRHAGIC CLOSED-HEAD INJURY

By

Dounya F. Jalloul



Makram Obeid, Assistant Professor
Department of Pediatrics and Adolescent Medicine

Advisor



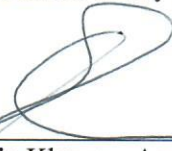
Hala Darwish, Associate Professor
Hariri School of Nursing

Co-Advisor



Marc Barakat, Assistant Professor of Clinical Specialty
Department of Psychiatry

Member of Committee



Samia Khoury, Associate Dean and Professor
Department of Neurology

Member of Committee



Firas Kobeissy, Associate Professor
Department of Biochemistry and Molecular Genetics

Member of Committee



Nada B. Lawand, Assistant Professor
Department of Neurology

Member of Committee

Date of thesis defense: September 16, 2019

AMERICAN UNIVERSITY OF BEIRUT

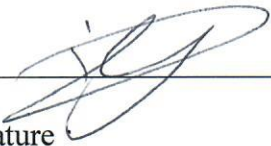
THESIS, DISSERTATION, PROJECT RELEASE FORM

Student Name: Jalloul Dounya Fouad
Last First Middle

Master's Thesis Master's Project Doctoral Dissertation

I authorize the American University of Beirut to: (a) reproduce hard or electronic copies of my thesis, dissertation, or project; (b) include such copies in the archives and digital repositories of the University; and (c) make freely available such copies to third parties for research or educational purposes.

I authorize the American University of Beirut, to: (a) reproduce hard or electronic copies of it; (b) include such copies in the archives and digital repositories of the University; and (c) make freely available such copies to third parties for research or educational purposes after : **One ---- year from the date of submission of my thesis, dissertation, or project.**
Two ---- years from the date of submission of my thesis, dissertation, or project.
Three --X years from the date of submission of my thesis, dissertation, or project.

 September 17, 2019
Signature Date

ACKNOWLEDGMENTS

This work, and all that is to come, is dedicated to my parents and my siblings. Thank you for always being a source of encouragement, reassurance, and support in all its forms.

Foremost, I would like to express my deepest gratitude to Dr. Makram Obeid for his constant support. Being part of your lab has been a cornerstone in my academic life, and it helped shape my critical thinking skills and guided me towards the type of researcher I would want to be.

I had the utmost privilege of working on a collaborative project between both the Epilepsy and the TBI teams. Thank you Dr. Hala Darwish and Dr. Firas Kobeissy for sharing your invaluable expertise in the behavioral and molecular aspects of TBI, and thank you Leila Nasrallah for your technical help throughout the project.

To the most wonderful lab managers, Yasser Medlej and Houssein Salah, thank you for your incredible patience in teaching me all needed skills, your constant uplifting and fun spirit, and your invaluable advice. Thank you Mouhamad El Darwish for always sharing your remarkable insights regarding the project, but also regarding all disciplines of science in its formal, natural, and social aspects.

To my labmates, Mariam Mouawia, Rita Asdikian, Farah Issa, Yara Mrad, Nancy Poladian, and Hadi Saredine, it was a great pleasure sharing laboratory work with you during the last year.

Lastly, a special *shout-out* to my dearest friends who have been my home away from home. Thank you for always challenging my opinions and for exposing me to the many ways of living. I am a different person because of each one of you.

AN ABSTRACT OF THE THESIS OF

Dounya Fouad Jalloul for Master of Science
Major: Neuroscience

Title: Characterization of Post-Traumatic Epileptiform Features and Behavioral Disturbances in a Clinically-Relevant Rodent Model of Hemorrhagic Closed-Head Injury

Background: Currently, there are no clinically available treatments to prevent traumatic brain injury (TBI)-related epilepsy, and the associated cognitive disturbances. Post-traumatic epilepsy (PTE) represents 20% of symptomatic epilepsies, and its incidence is reported to be as high as 53% after severe head injury. The pediatric population is particularly at risk given the developmental consequences of TBI, even after non-penetrating closed-head injuries that account for 75% of all TBI cases. Investigating new drugs has been hindered by the low rate of seizure emergence in available rodent models (as low as 3% in open head injuries). Hemorrhage, among others, constitutes an important risk factor for PTE. Therefore, we hypothesize that producing a traumatic lesion with a substantial hemorrhagic component will lead to higher rates of PTE emergence in a rodent TBI model. In this study, we used a modified controlled cortical impact (CCI) TBI model where bleeding is promoted with a pre-impact single heparin injection. The partial sacrifice of construct validity with the use of heparin aims at improving the face validity of increasing PTE rates; a common scenario in most rat seizure models that rely on the administration of chemicals. Following closed-head hemorrhagic TBI, we investigated PTE and cognitive deficits, two of the most clinically-relevant outcomes of TBI.

Methods: Closed-TBI was induced in postnatal day 35 (P35) male Sprague-Dawley rats using the modified CCI model, targeting the skull overlying the right parieto-temporal area. Prior to injury induction, each rat received an intraperitoneal heparin injection (600 IU/Kg) in the CTBIHP group (closed-TBI with heparin, n=11) or a volume matched injection of normal saline in the CTBINS group (closed-TBI with normal saline, n=14). Weight-matched control littermates were sham manipulated and received either heparin in the HP group (control with heparin, n=8) or normal saline in the NS group (control with normal saline, n=10). Continuous epidural EEG recordings were obtained 2 weeks post-TBI for one month (P50-P80). The rats were then sequentially subjected to the Morris water maze MWM (hippocampal-dependent spatial navigation), rotarod test (motor function), modified active avoidance MAAV (recognition and avoidance of auditory-signaled and context-cued electrical foot-shock), and Von Frey and Hargreaves tests (sensory function). Following behavioral tests, EEG was obtained for an additional one month (P100-130). EEG recordings were reviewed to assess the frequency of seizures, spikes, and polyspikes. Glial fibrillary acidic protein (GFAP)

levels and neuronal density were assessed on histological sections in the hippocampus and the parietal cortex at P37 and P130, respectively.

Results: Following TBI, rats that received heparin prior to the impact, developed more prominent hemorrhage ipsilateral to the impact site, compared to non-heparinized rats. No skull fractures were observed and there were no mortalities. Continuous long-term EEG recordings revealed a higher number of spikes at the beginning of recording, 2 weeks post-TBI, in all heparinized CTBIHP rats (48.911 ± 5.623 spike/hour) compared to the CTBINS group (16.46 ± 1.867 spike/hour, $p < 0.05$). The number of spikes decreased over time in both groups and plateaued in frequency 3 months post-TBI, while remaining higher in the heparinized TBI rats ($p < 0.05$). Spikes were not found in the control groups. Polyspikes were detected in all groups but were significantly more abundant in the CTBIHP (30.297 ± 3.413 polyspike/hour, $p < 0.05$) and CTBINS (19.777 ± 1.621 polyspike/hour $p < 0.05$) groups compared to the HP (0.943 ± 0.124 polyspike/hour) and NS (0.576 ± 0.134 polyspike/hour) control groups. Polyspikes frequency decreased and plateaued over time, with the CTBIHP group maintaining a significantly higher frequency ($p < 0.05$). In the MAAV test, retention of contextual learning was lower in the CTBIHP ($36.29 \pm 13.83\%$, $p < 0.05$) and CTBINS ($55.35 \pm 11.79\%$, $p < 0.05$) rats compared to NS ($90.62 \pm 2.004\%$) and HP ($79.47 \pm 14.06\%$) controls. There was no difference among the 4 groups in avoidance of context-cued or tone-signaled shocks and in the retention of auditory learning. In the MWM, all groups learned to reach the invisible escape platform during the 5 training days, yet both TBI groups were slower (longer escape latency) than the controls on day 3 (ANOVA $p < 0.05$). All groups had comparable performance in the sensorimotor tests (Rotarod, Von Frey, and Hargreaves). The levels of GFAP were higher in the injured rats ($p < 0.05$) than the controls, 48 hours post-TBI. Moreover, the CTBIHP had significantly higher GFAP levels ($p < 0.05$) than CTBINS in the right hippocampus (ipsilateral to the injury site). Three months post-injury, neuronal loss was comparable in both TBI groups and was similar in both left and right hippocampi (CTBIHP = 830 ± 75 cell/mm²; CTBINS = 879 ± 23 cell/mm²). There was no neuronal loss in the NS (1389.129 ± 93 cell/mm²) and HP (1390.556 ± 95.5 cell/mm²) control groups.

Conclusions: The persistence of spikes in TBI groups suggest the emergence of a permanent abnormal hyperexcitable network which may behaviorally manifest with seizures on the long run. Prominent bleeding further exacerbated the injury and contributed to more pronounced hyperexcitability, pointing to the potential role of hemorrhage in PTE emergence mechanisms. In addition, our preliminary data suggest that TBI groups displayed hippocampal deficits and learning difficulties in both the Morris water maze and in contextual conditioning. Ongoing studies aim at extending the duration of EEG recording for several months given the long latency period of PTE emergence in both humans and rodents, and at investigating the mechanisms underpinning the observed hyperexcitability and cognitive problems, in order to fully characterize our model as a platform for studying PTE and its potential biomarkers and treatments.

CONTENTS

ACKNOWLEDGMENTS	V
ABSTRACT	VI
LIST OF ILLUSTRATIONS	XI
LIST OF TABLES	XII
LIST OF ABBREVIATIONS	XIII
Chapter	
I. INTRODUCTION	1
A. Traumatic Brain Injury	2
1. TBI Clinical Burden	2
2. TBI Classification	3
a. Mechanistic Classification	4
b. Other Classifications	5
3. TBI Pathophysiology	7
4. TBI Comorbidities	9
a. Cognitive Disturbances	10
b. Seizures and Epilepsy	11
B. Post-Traumatic Epilepsy	11
1. Epilepsy	12
2. Epileptogenesis	14
3. Risk Factors	16
a. Hemorrhage	17
b. Other Risk Factors	18
C. Modeling PTE Using TBI Rodent Models	19
1. TBI Animal Models	19
a. The Fluid Percussion Injury (FPI)	19
b. The Controlled Cortical Impact (CCI)	20

2. Challenges in PTE Modeling and Available Studies	21
D. Differences in the Coagulation Profile Between Humans and Rats	27
II. AIMS AND HYPOTHESES.....	29
III. MATERIALS AND METHODS.....	31
A. Animals and Experimental Design	31
B. Closed-Head Traumatic Brain Injury Induction	32
C. Surgical EEG Electrodes Implantation and EEG Recordings	33
D. Behavioral Panel.....	35
1. Morris Water Maze (MWM)	36
2. Rotarod	37
3. Modified Active Avoidance (MAAV)	38
4. Sensory Tests: Von Frey and Hargreaves	40
E. Euthanasia and Cardiac Perfusion Surgery	41
F. Immunohistochemistry for GFAP and NeuN.....	41
G. Statistical Analysis.....	43
IV. RESULTS	44
A. Closed-head TBI induction with prominent hemorrhage	44
B. EEG findings: increased hyperexcitability after hemorrhagic closed-head TBI.....	45
C. MWM: visuospatial navigation.....	49
D. Rotarod: motor performance.....	50
E. MAAV: recognition of auditory-signaled and context-cued shocks and acquisition of adaptive behavior	50
F. Von Frey and Hargreaves: sensory pathways integrity	52
G. Histological Analyses	52
V. DISCUSSION	56

VI. LIMITATIONS AND FUTURE PERSPECTIVES	62
REFERENCES	63

LIST OF ILLUSTRATIONS

Figure	Page
1. TBI classification	4
2. Closed-head injury	6
3. Comorbidities of TBI	10
4. Seizures and epilepsy classification	13
5. Epileptiform discharges	17
6. Hemorrhage following TBI.	18
7. Experimental design of the project	31
8. Electrodes implantation surgery	34
9. Initiating of EEG recordings	35
10. EEG recording epochs	35
11. Morris water maze	37
12. Modified active avoidance	39
13. Post-TBI hemorrhage and post-surgery recovery time	44
14. Spikes in TBI rats	46
15. Quantification of spikes.	47
16. Polyspikes	48
17. Quantification of polyspike.	48
18. Visuospatial navigation in the Morris water maze.	49
19. Rotarod performance.	50
20. Avoidance of tone-signaled and context-cued electrical foot-shocks	51
21. Paw withdrawal response to mechanical and thermal stimuli.	52
22. GFAP immunostaining.	54
23. NeuN immunostaining.	55

LIST OF TABLES

Table	Page
1. Different electrographic definitions and seizure duration cutoff in PTE studies .	23
2. PTE studies using the CCI rodent TBI model	24
3. PTE studies using the FPI rodent TBI model	25
4. PTE studies using different TBI models.....	26

LIST OF ABBREVIATIONS

AHT	Abusive head trauma
AMPA	α -amino-3-hydroxy-5-methyl-4-isoxazolepropionic acid
CA	Cornu Ammonis
CCI	Controlled cortical impact
CHI	Closed-head injury
CTBIHP	Closed-TBI with heparin (TBI group)
CTBINS	Closed-TBI with normal saline (TBI group)
DAI	Diffuse axonal injury
DG	Dentate gyrus
EEG	Electroencephalography
FPI	Fluid percussion injury
GABA	<i>gamma</i> -Aminobutyric acid
GCS	Glasgow coma scale
GFAP	Glial fibrillary acidic protein (astrocyte marker)
HP	Heparin (control group)
KA	Kainic acid
KAR	Kainic acid receptor
MAAV	Modified active avoidance
MWM	Morris water maze
NeuN	Neuronal nuclei (neuronal marker)
NMDA	<i>N</i> -methyl-D-aspartate
NS	Normal saline (control group)
P	Postnatal days
PTA	Post-traumatic amnesia
PTE	Post-traumatic epilepsy
SDH	Subdural hemorrhage
TBI	Traumatic brain injury

CHAPTER I

INTRODUCTION

PROLOGUE

Traumatic Brain Injury (TBI) is a form of acquired brain damage caused by an external mechanical force, such as falls, car accidents, or sudden hit by moving or stationary objects [1]. TBI-induced epilepsy, known as post-traumatic epilepsy (PTE), can be considered as one of the most debilitating outcomes of TBI given how it can further exacerbate brain damage and contribute to behavioral disturbances. The emergence of cognitive deficits and spontaneous seizures is reported throughout the entire spectrum of TBI severities, especially in the susceptible pediatric and adolescent populations [2-4]. Rates of TBI tend to peak in children (0-4 years old) and adolescents (15-19 years old) [5]. First, children younger than 5 years old are at risk to sustain abusive head trauma (AHT) caused by blunt impact or violent shaking, which may have severe consequences on their mental development [6]. Moreover, falls account for the majority of emergency department visits causes in kids (0-17 years old) [5]. Even mild repetitive impacts caused by sports and recreational activities have been proven to have long-term cognitive and emotional effects on young children [7]. It is important to note that all these injuries are closed-headed in nature, meaning they impact the skull and do not directly breach the dura mater and penetrate the brain. Penetrating injuries might have a worse prognosis, but they are relatively rare, and it is non-penetrating closed-head injuries that represent the majority of all TBI cases and can also have detrimental effects [5, 8]. Therefore, in this study, we aim to focus on the consequences of closed-head injury in the pediatric population, especially epilepsy and long-term behavioral

disturbances. We are using a rodent model of closed-head TBI, given that most available PTE studies in rodents use models of open-head injuries which does not reflect the majority of TBI clinical cases. We are also focusing on hemorrhage being a significant risk factor for PTE, taking into consideration the interspecies differences in the coagulation profile between humans and rats, with rats being less prone to bleeding [9].

A. Traumatic Brain Injury

TBI is characterized by both morphological and physiological changes, where it can cause disturbances at the level of the cellular integrity and affect the homeostasis of the brain tissues and cell functionality, thus, causing cellular dysfunction [10].

Clinically, TBI can cause long-term neurological deficits and cognitive disturbances, depending on severity and location.

1. TBI Clinical Burden

TBI is considered a major health concern worldwide, with a global annual incidence of 331-412 cases per 100,000 individuals [11]. As a ‘silent epidemic’, it is estimated that 64-74 million people will sustain TBI worldwide every year from various types and severities [12], with an economic burden of 400 billion USD annually [13]. TBI is estimated to surpass many diseases as the primary cause of death and disability by 2020 [14]. In the Middle East and North Africa (MENA) region, war conflicts and terrorism are a major cause of TBI, with an incidence of 340-528 cases per 100,000 [11]. Lebanon, like most developing countries, also suffers from violence due to political instability. War and blast injuries, mainly due to the Lebanese-Israeli conflict,

contribute to a large number of TBI cases [15]. Moreover, the 2012 National Health Statistics Report estimated an annual incidence of 100,000 cases of motor vehicle accidents, in a population that does not exceed 4 million citizens. A retrospective study at the American University of Beirut Medical Center (AUBMC) showed that falls (38.2%) were the most common type of injuries, followed by penetrating/gunshot injuries (14.8%), and road traffic accidents (11.8%) [16].

The highest rates of TBI tend to peak in children (0-4 years old), adolescents/young adults (15-24 years old), and elderly (> 60 years old) [5]. Compared to their adult counterparts, the pediatric population warrants particular concern given the developmental consequences of early brain injury. Indeed, TBI is the leading cause of death and long-term disability in children [17-20], and one of the most common reasons for interrupted normal brain development [21-28]. Mild TBI constitutes 80% of children head injuries, and up to 90% of all injuries are associated with normal imaging [29]. However, even when no lesions are visible on MRI, children who have sustained a head injury suffer from long-term intellectual and cognitive impairment [26].

2. TBI Classification

Head Injuries can be classified based on different criteria [30] (Figure 1), such as the mechanism of injury (penetrating vs. non-penetrating), the severity (mild, moderate, severe), and the extent of the structural damage (focal vs. diffuse).

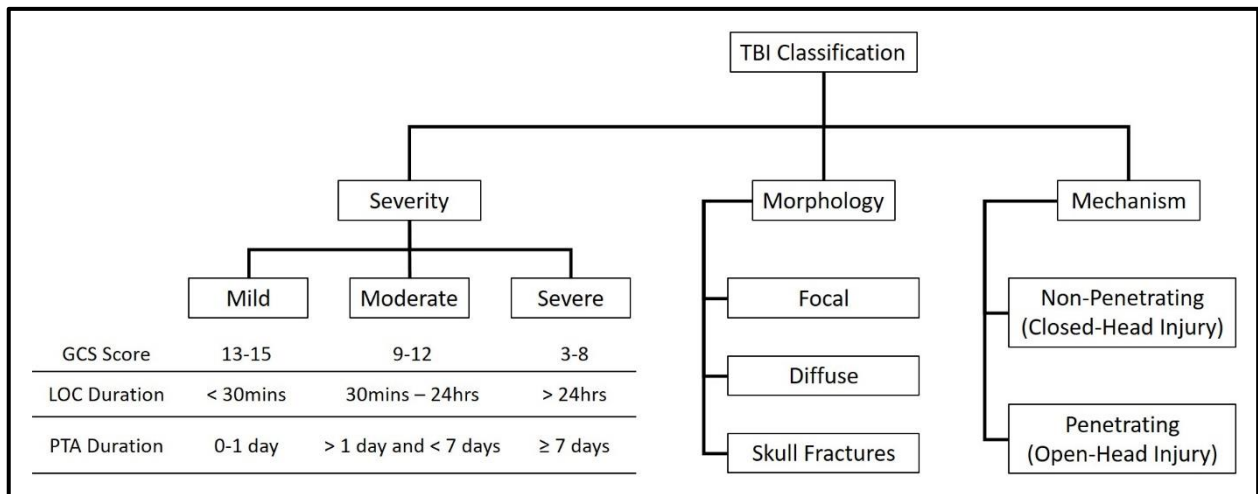


Figure 1. TBI classification. For clinical assessment, TBI can be classified according to the mechanism of injury, the extent of the injury, or the clinical severity. (GCS= Glasgow coma scale; LOC= loss of consciousness; PTA= post-traumatic amnesia).

a. Mechanistic Classification

TBI can be classified based on the mechanism by which the patient was injured. In this regard, TBI can be either a closed-head (non-penetrating) or an open-head (penetrating) injury. *Open-head injuries* are often a neurosurgical emergency and may cause permanent disabilities or death [31]. TBI is classified as a penetrating injury when an object breaches the dura and directly damages the brain [32]. They are caused by high-velocity objects, such as bullets or shell fragments, or by low-velocity objects, like knives or bone fragments from a skull fracture. Penetrating head injuries have a worse prognosis than non-penetrating closed-head injuries; however, they are rare and do not represent the majority of TBI cases [8].

On the other hand, *closed-head injuries (CHI)* are the most common type of TBI, and they usually describe blunt injuries caused by falls, assaults, or vehicle accidents, in which the skull remained intact, and the dura was not breached [33]. Although the brain is not directly hit, closed-head injuries can lead to concussion, intracranial hemorrhages, and diffuse axonal injury, all of which can have detrimental physical and behavioral consequences [34-38]. According to the Center of Disease of

Control (CDC) [5], falls account for 52% of TBI causes in the United States, and represent 49% of TBI-related emergency department visits in the pediatric and adolescent population (0-17 years old). Other causes include motor vehicle accidents (20%), and being struck with or against an object (17%) [5]. The impact causes *coup* injury that occurs under the site of the hit with an object, and if the force is great enough, it can make the brain move in the opposite direction leading to a *contrecoup* injury on the opposite side [39]. Coup and contrecoup injuries are associated with discrete focal brain contusions (bruising of brain tissue). Closed-head injury can also be caused by *acceleration-deceleration* force in which the head is accelerated and then stopped suddenly (i.e., car accidents) [39]. Acceleration-deceleration trauma may occur unaccompanied by impact (i.e., babies who are violently shaken and suffer from abusive head trauma, AHT). When the impact causes the brain to move within the cranium at a different velocity than the skull, *rotational trauma* can occur and result in shearing of axons [39]. Another example of CHI is the sport-related injuries and their consequences which have gained a heighten interest recently, with an estimation of 3.8 million cases per year occurring at all ages in the US alone [7]. According to the American Academy of Pediatrics, up to 1.9 million of these cases occur in children younger than 18 years old [40].

b. Other Classifications

Another dichotomous TBI classification is into the *primary* injury that happens seconds to minutes after TBI, and the *secondary* injury that is the gradual damage caused by a cascade of cellular events that can further exacerbate the consequences of the initial insult [41]. TBI is additionally classified into *focal* or *diffuse* injury. Focal

injury is restricted to a specific area and can include focal contusions, lacerations, and hematomas. The symptoms are usually related to the damaged area (e.g., aphasia after damage to Broca’s area). Diffuse injury is a widespread injury that affects multiple brain regions (multifocal), and it includes hypoxic/ischemic injury, vascular damage, brain swelling (edema), and diffuse axonal injury (DAI) [42].

Moreover, brain injuries can be classified based on clinical severity into mild, moderate, or severe, mostly according to the Glasgow Coma Scale (GCS) [43]. The

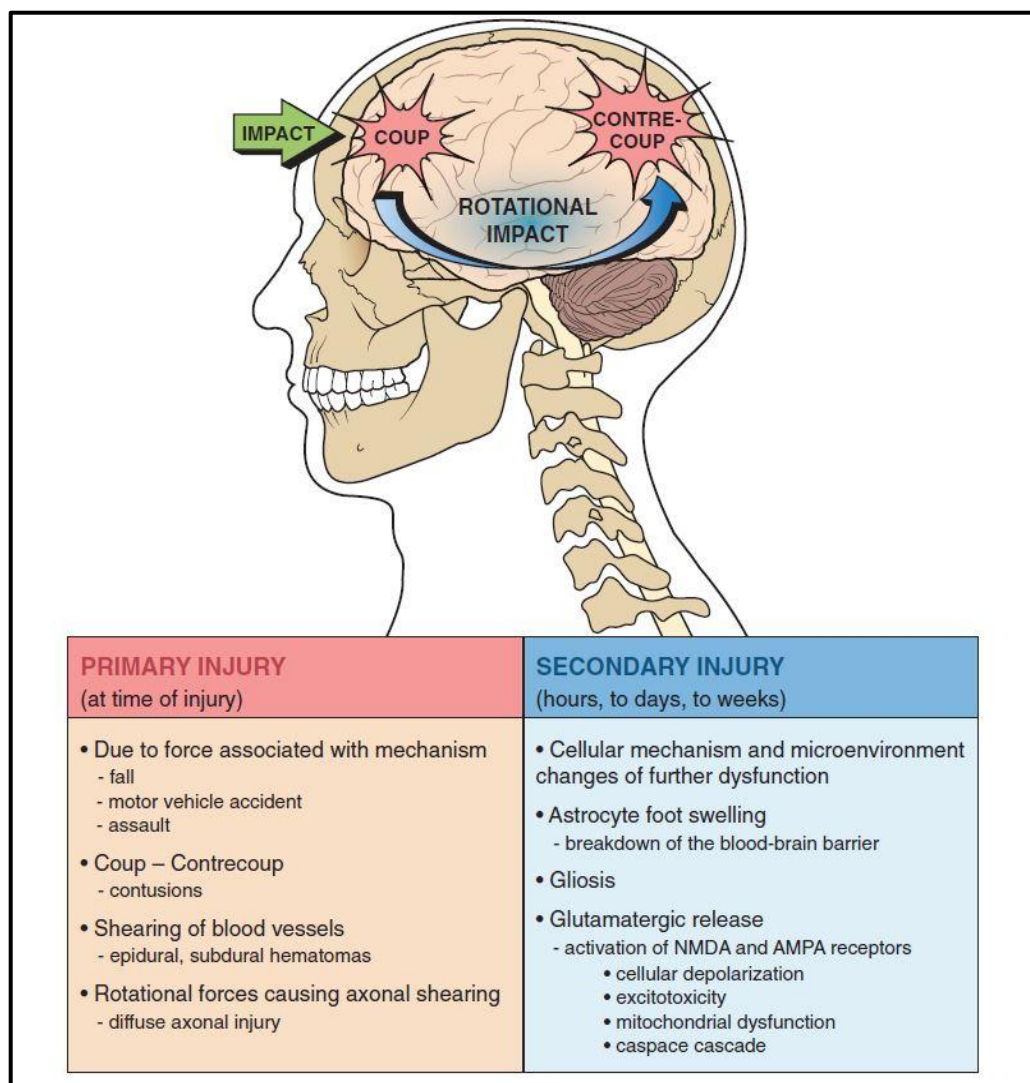


Figure 2. Closed-head injury. Schematic of injury mechanisms that occur due to head trauma. (Figure adapted from Bales et al. [33]).

GCS score is measured based on the patient's motor, verbal, and eye-opening responses to a stimulus. Other factors are used to help in determining severity, such as post-traumatic amnesia (PTA) and loss of consciousness (LOC) duration. In general, mild TBI has a GCS score of 13 or above, and it accounts for around 80% of TBI cases [44]. Moderate TBI (GCS 9-12) and Severe TBI (GCS 3-8) can lead to prolonged or permanent severe neurological problems.

3. TBI Pathophysiology

The pathogenesis of TBI is a multidimensional process that involves multiple systems interactions. Primary injury occurs in milliseconds during TBI and is characterized by tissue damage and impaired regulation of blood flow and metabolism. What follows is a cascade of molecular and inflammatory reactions, known as the secondary injury, that further exacerbate the damage. The myriad of cellular and physiological factors leads to the depolarization of neurons and an excessive release of excitatory neurotransmitters (mainly glutamate), triggering a cascade of pathological events known as excitotoxicity [45]. Glutamate's extracellular concentration can increase up to 50 folds in humans following TBI, and it eventually leads to a massive influx of calcium and sodium [46]. Disruption of calcium homeostasis sequentially activates a series of mechanisms resulting in mitochondrial dysfunction, oxidative stress, and neuronal death [47]. Glial cells, particularly microglia, will play a critical role as the first line of defense to promote neuro-restorative processes by producing anti-inflammation factors (M2 phenotype). However, microglia can also display a pro-inflammation state (M1 phenotype). Consequently, neuroinflammation can become maladaptive over time and the brain can stay in a prolonged state of inflammation for

years after TBI, hindering brain repair mechanisms and contributing to long-term physical and behavioral problems [48-50]. Astrocytes are also key players in the multicellular response to TBI. They are crucial for the maintenance of healthy brain functions (e.g., neurotransmitters buffering, blood flow regulation, synaptic function regulation, energy provision). Upon brain injury, astrocytes undergo several changes in their function, morphology, genetic expression, and proliferation capacity. These changes are collectively referred to as reactive astrogliosis [51]. Astrogliosis is important for brain repair mechanisms and can protect undamaged areas from the secondary injury by forming a protective “scar” and sealing off the injured tissue. However, it can become maladaptive, and reactive astrocytes can lose their homeostatic functions and contribute to the emergence and the progression of many neurological diseases [52]. Furthermore, damage to neuronal axons (shearing, stretching or twisting) can lead to diffuse axonal injury (DAI), mainly seen at the junction between the grey and white matter as the axons enter the dense (myelinated) and less-fluid filled white matter. DAI can persist for years after TBI [53], even after chronic mild injuries [54, 55]. Degeneration of axons and the sprouting of new aberrant ones can modify the connections within the circuitry and permanently change brain networks. The countless mechanisms involved in the secondary injury can lead to permanent changes in the brain, disrupting its internal homeostasis. One of these possible changes is the net shift of the electrophysiological balance toward hyperexcitability, and the development of aberrant networks capable of seizure emergence, a process known as epileptogenesis (Section I-B.2).

All these mechanisms will collectively lead to a variety of comorbidities, depending on injury characteristics and the patient's personal traits, which make TBI a life-long disease and a leading cause of worldwide disability.

4. TBI Comorbidities

TBI is a multifactorial condition which consequences highly depends on the injury's location, type, severity, and extent (Figure 3). Comparison and prediction of outcomes are further complicated by the heterogeneity within the affected population. Severe TBI has a worse prognosis, with a mortality rate of 39% [56]. Survivors have a lower life expectancy than the general population and suffer from long-term physical, cognitive, and psychological impairments that can profoundly affect their lifestyle and independence, along with their relationships and employment [57]. TBI can cause location-specific symptoms that directly reflect the affected brain areas or networks (e.g., aphasia, sensorimotor deficits, and visual impairments). Additionally, prolonged secondary injury may eventually lead to neurodegenerative diseases such as Alzheimer's Disease, Parkinson's Disease, and Amyotrophic Lateral Sclerosis [58]. In addition to the physical and somatic comorbidities, numerous psychiatric disorders, including mood, anxiety, and substance-use disturbances are associated with TBI, even after minor head injuries [59-62]. However, the ensuing cognitive disturbances, in addition to the risk of chronic emergence of unprovoked seizures, a condition known as post-traumatic epilepsy (PTE), can be considered the most clinically-significant comorbidities of TBI because they can strongly affect all aspects of the patient's life.

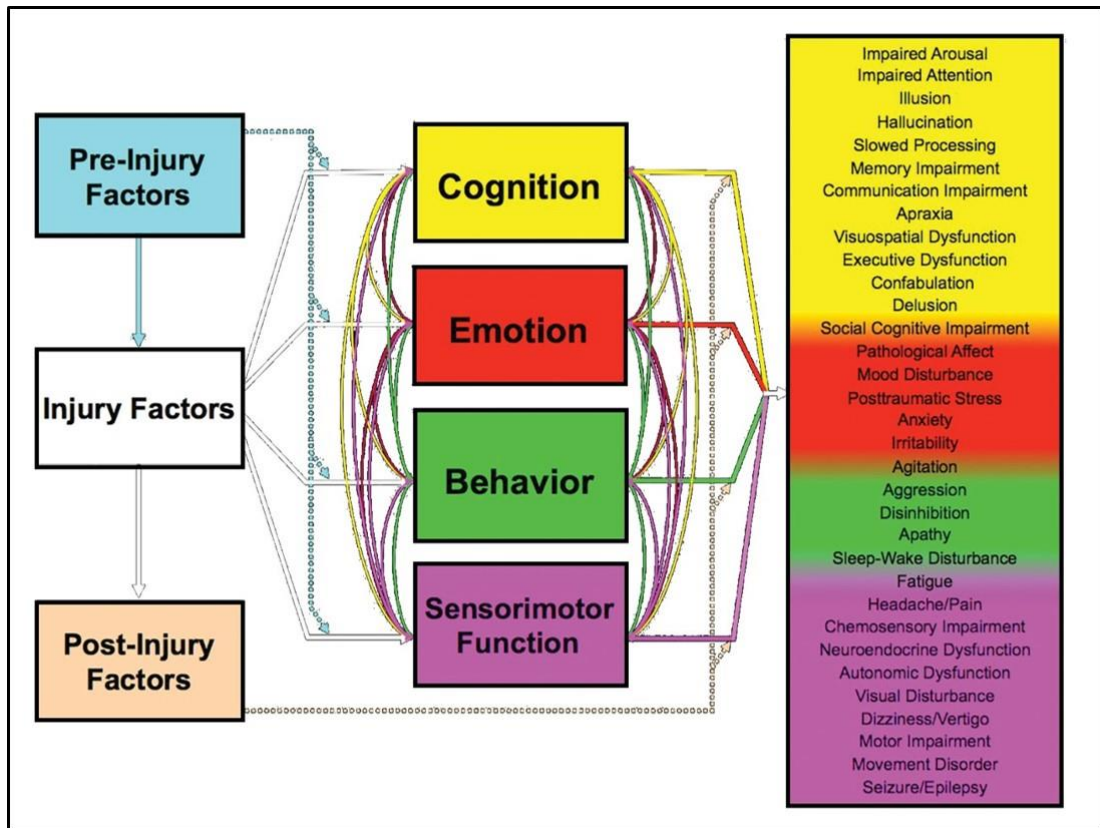


Figure 3. Comorbidities of TBI. Outcomes of TBI are affected by pre-injury factors (age, sex, preexistent personal conditions etc...), by injury mechanisms (severity, secondary cascades etc...), and by post-injury factors (hospitalization time, rehabilitative interventions etc...). Disturbances in one of the domains of sensorimotor, cognitive, emotional, and behavioral functions entail disturbances in the others. Collective interactions of all these factors give rise to post-traumatic symptoms and conditions. (Figure adapted from Arciniegas et al. [59]).

a. Cognitive Disturbances

Cognitive impairments are among the most debilitating sequelae of TBI across the entire spectrum of severities. Cognition is the term attributed to the range of the mental processes involved in attention, learning, memory, and executive functions, among others [63]. These functions are vital for school and job performances, social relationship, and independent daily living, and thus, they can critically affect the quality of life. Cognitive deficits can be immediate and transient (e.g., post-traumatic confusional state, post-traumatic amnesia PTA), but can also be delayed, evolving, and permanent [64]. In children and adolescents, TBI can lead to developmental problems associated with the domains of intellectual and planning abilities, communication,

problem-solving, social skill, self-care abilities, and visual functions [21-23, 25, 26, 28]. The pediatric population is, furthermore, also susceptible to develop attention deficiency and hyperactivity disorder (ADHD) after TBI [65].

b. Seizures and Epilepsy

One of the leading causes of TBI-related morbidity is the emergence of chronic spontaneous recurrent seizures, known as post-traumatic epilepsy (PTE). Seizures are electro-clinically defined as paroxysmal electrographic rhythmic evolving patterns accompanied by consistent stereotypical behaviors (Section I-B). However, seizures can also be strictly electrographic. PTE represents 10 to 20% of symptomatic epilepsies, and 5-10% of all epilepsies [66]. The risk of seizure emergence depends on the injury's severity and can vary between 7% and 40% after closed-head injury, and be as high as 53% after penetrating head injury [67]. The underlying mechanisms of this condition are still poorly understood, and unfortunately, currently available animal models of PTE suffer from many challenges that are hindering better characterization of PTE mechanisms (Section I-C.2).

B. Post-Traumatic Epilepsy

Post-Traumatic Epilepsy (PTE) refers to the chronic emergence of unprovoked seizures after a head trauma (> 1 week post-TBI), and it is to be distinguished from immediate provoked seizures that happen in the acute phase following TBI. The time between the injury and the emergence of the first late spontaneous seizure (the latency period) can span anywhere between a few weeks to a few years (up to 20 years).

Approximately 75% of PTE cases occur within the first 2 years after TBI [68]. The risk of recurrence after one late seizure is around 70%, and thus, the emergence of a single late seizure post-TBI is considered sufficient for the diagnosis of PTE [69].

A “seizure” is a paroxysmal disruption of neurological functions, caused by the excessive hypersynchronous firing of brain neurons [70]. It electrographically manifests as a rhythmic pattern of spikes and sharp-waves, evolving in time and space. An electrographic seizure may behaviorally manifest as subjective sensations (e.g., tingling, buzzing, smells, and hallucinations) and uncontrolled muscle activity that can culminate into rhythmic clonic or tonic stiffening, known as convulsions [71]. While seizures may transiently occur following acute reversible incidences (fever, hypoglycemia), they can have a chronic recurrence due to an innate (genetic) or an acquired epileptogenic network (e.g., stroke, TBI), leading to a condition known as “epilepsy”.

1. Epilepsy

The oldest known detailed account of epilepsy dates back to 2000 B.C. [72]. Seizures have long been considered a supernatural phenomenon associated with evil spirits overtaking the body, and in Greek, “*epilepsia*” literally means “to possess” or “to seize” [73, 74]. It was not until 400 B.C. that Hippocrates attributed epilepsy to a physiological origin instead of a divine one, a rather revolutionary view discussed in his book (putative) “On the Sacred Disease” [74]. Unfortunately, epilepsy remained associated with the older superstitious view for the next 2000 years and was approached with fear, suspicion, and social stigma [75]. Hippocrates’ standpoint only started to take root in the 18-19th centuries, and laws discriminating against epilepsy patients weren’t

amended until the 1970s in the UK and the USA [76]. Current global efforts to raise awareness about epilepsy helps bring the disease “out of the shadows”, and aims to improve care and reduce the disease’s impact. The Global Campaign Against Epilepsy is led by the World Health Organization (WHO), the International League Against Epilepsy (ILAE), and the International Bureau for Epilepsy (IBE).

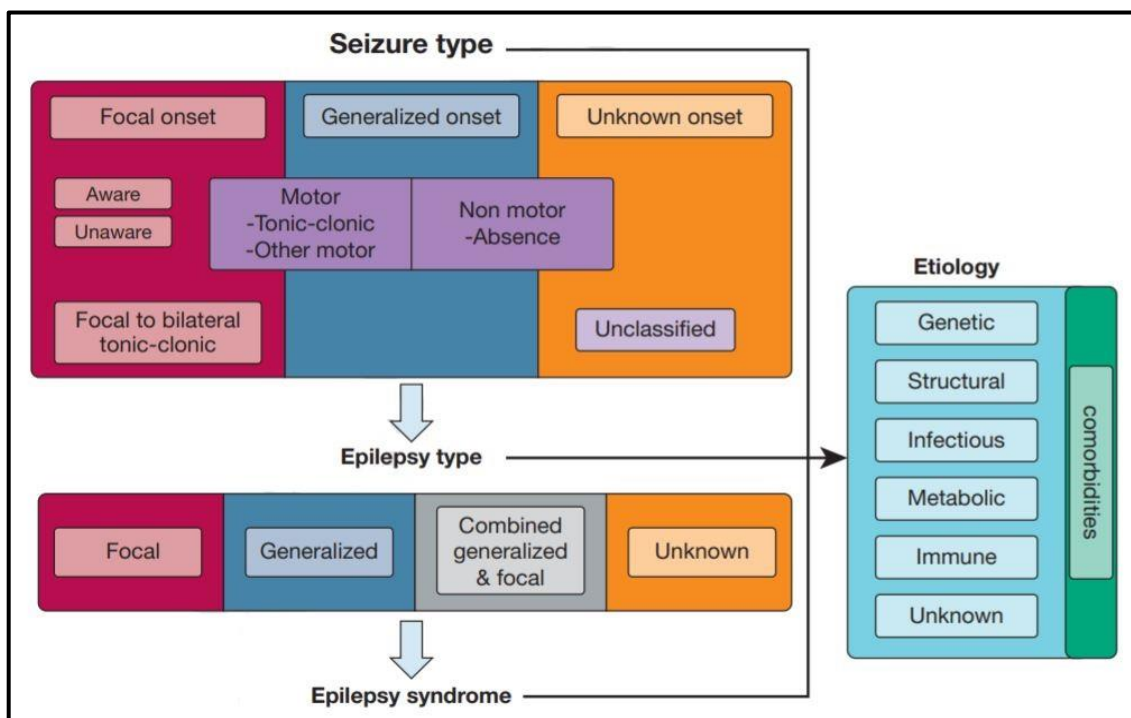


Figure 4 . Seizures and epilepsy classification. Operation classification of seizure types according to the International League Against Epilepsy (ILAE) [78]. (Figure adapted from Somboon et al. [79]).

Epilepsy is the most common neurological disease worldwide, affecting more than 50 million people [77]. 75% of cases being at childhood, highlighting the susceptibility of the developing brain to seizures [71]. Epilepsy can be classified by etiology, but also electro-clinically based on the accompanying signs and symptoms (Figure 4) [78, 79].

Normal brain functions heavily rely on the electrophysiological balance between the excitatory (mainly via glutamatergic signaling) and the inhibitory mechanisms (mainly via GABAergic signaling) in the brain [71]. This electrophysiological homeostasis is primarily maintained by the inhibitory channels of GABA_A ionotropic receptors, and by the NMDA, AMPA, and KAR receptors of glutamate [80]. The disruption of this delicate balance leads to an array of pathologies, with seizure emergence as a prime example of a net shift toward hyperexcitability. Seizures can result from genetic or acquired alternations at different levels of brain functions. Genetic pathologies can include anything from the circuit level (e.g., abnormal neurons network in cortical dysplasia), to the receptor and channel levels (e.g., abnormal GABA receptor subunits, and K⁺ channel mutation). Similarly, acquired head insults such as TBI can cause abnormal network reorganization (e.g., altered hippocampal circuitry). Moreover, even the normally developing brain is naturally more susceptible to seizures since the excitatory synaptic functions develop before the inhibitory ones, and GABA causes excitation during early life rather than inhibition [81, 82].

2. Epileptogenesis

Epileptogenesis is a chronic process, triggered by genetic or acquired factors, that refers to the development of an aberrant brain network with an increased seizure susceptibility capable of generating spontaneous recurrent seizures, resulting in the development or the progression of an epileptic condition [81]. Epileptogenesis is not limited to the latent period as previously believed but can continue indefinitely beyond the initial unprovoked seizure.

On the cellular level, epileptic networks seem to be characterized by excitatory positive feedback and the feature of bistability, which is the capacity to switch between normal and epileptic activity [81, 83]. Although the mechanisms underlying this positive feedback are not yet fully understood, it can be generally discussed as changes in the excitatory circuits and the inhibitory circuits. Following TBI, the brain initiates “self-repair” mechanisms to promote functional recovery, including angiogenesis, gliosis, neurogenesis, axonal sprouting, and synaptic circuitry remodeling [41]. Many brain regions seem to be susceptible for network reorganization after an injury, most particularly the hippocampus and the neocortex. The dentate gyrus of the hippocampus served as a model system of excitatory axonal sprouting. Dentate granular cells, normally not interconnected, sprout abnormal axonal collaterals into the inner molecular layer of the dentate, a phenomenon known as mossy fiber sprouting, and form excitatory connections with neighboring granular cells, thus contributing to abnormal network synchronization [41, 81]. Other changes in functional excitability have been observed in experimental models, independent of mossy fiber sprouting. These changes include an increase in spontaneous burst discharges in the neocortex which appear to be associated with an increase in excitatory synapses onto pyramidal neurons. Additionally, pyramidal neurons of the CA1 (cornu Ammonis) region of the hippocampus show immediate deafferentation following experimental TBI, probably due to a loss of CA3 neurons that is followed by an increase of synaptic contacts and fiber excitability [84, 85].

Changes in inhibitory circuits are also involved in epileptogenesis. One possibility is that the loss of an inhibitory circuit uncovers a preexistent positive feedback [86]. For example, the loss of hilar interneurons in the dentate gyrus that

usually excite the inhibitory basket cell interneurons has been associated with a decrease of synaptic inhibition of granule cells [87-90]. Furthermore, alternations in the expression levels of GABA_A receptor subunits have been demonstrated following injury in rodents and might contribute to inhibition disturbances [91, 92].

All of the aforementioned network changes and the net shift toward hyperexcitability can lead to the emergence of epileptic discharges that may eventually manifest with seizure emergence [93] (Figure 5). Epileptic discharges include spikes, polyspikes, and spike-wave discharges, among others. Spikes are brief paroxysmal discharges of < 250 milliseconds duration that can be detected on both the scalp EEG and the cortical EEG (ECoG) [94]. They arise from the synchronous activation of neurons [95], and seem to play a role in epileptogenesis by inducing axonal sprouting and forming excitatory connections [96, 97]. These changes at the levels of the connections can contribute to transient cognitive impairments, such as alterations at the level of memory retrieval [98]. Indeed, it has been shown that spikes in humans can interfere with neural processing and memory and affect the functions within the brain region in which they occur [99-103]. In the clinical setting, spikes have a diagnostic importance in temporal lobe epilepsy [104] and in outcome prediction of seizure surgeries [105, 106].

3. Risk Factors

Given the variable latency and the unpredictability of PTE emergence, many efforts are put into identifying the risk factors associated with a higher risk of PTE. These factors include, among others, intracranial hemorrhage, early seizure, and skull fractures.

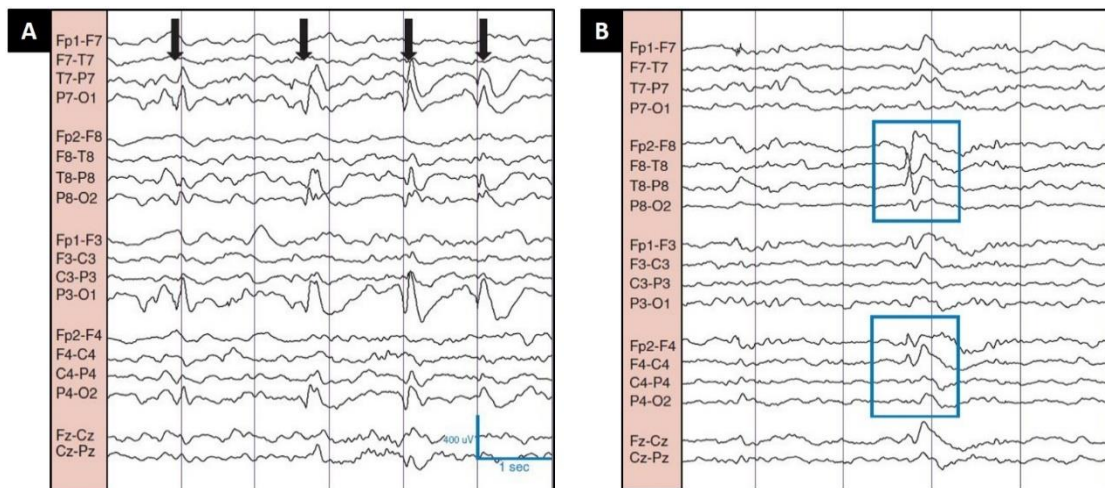


Figure 5. Epileptiform discharges. Occipital spikes (Panel A) and frontotemporal sharp waves (Panel B) detected on the EEG of epilepsy patients. (Figure adapted from Marcuse et al. 2016 [93]).

a. Hemorrhage

Intracranial hemorrhages are a serious aftermath of TBI, and they call for an immediate surgical consideration [107] (Figure 6). Intracranial hemorrhages of different varieties (epidural, subdural, subarachnoid, and intracerebral) affect 25-45% of severe TBI cases, and 3-12% of non-severe TBIs [33]. Several clinical studies reveal a correlation between trauma-induced hemorrhage and a higher risk of PTE development, with subdural hemorrhage (SDH) being the most associated with PTE (up to 85% of PTE patients have had an SDH at impact time) [108-110]. SDH can be life-threatening because it leads to an increase of the intracranial pressure that causes the compression and damage of soft brain tissue, contributing to epileptogenesis in the damaged area. One mechanism by which hemorrhage can induce epileptogenesis is via the release and deposition of iron and hemosiderin after the breakage of hemoglobin [111, 112]. The autoxidation of iron can lead to the formation of free radical intermediates and reactive oxygen species (ROS) that are believed to contribute to the mechanisms of seizure emergence [113, 114]. In a population-based study of 1885 cases, the risk ratio (RR) of

seizures after TBI was high with brain contusion (RR=5.9), but this risk was seven-fold higher when combined with intracranial hemorrhage (RR=42.6) [115]. Although prominent bleeding following TBI is a significant risk factor of PTE, controlling it in TBI experimental settings is very challenging.

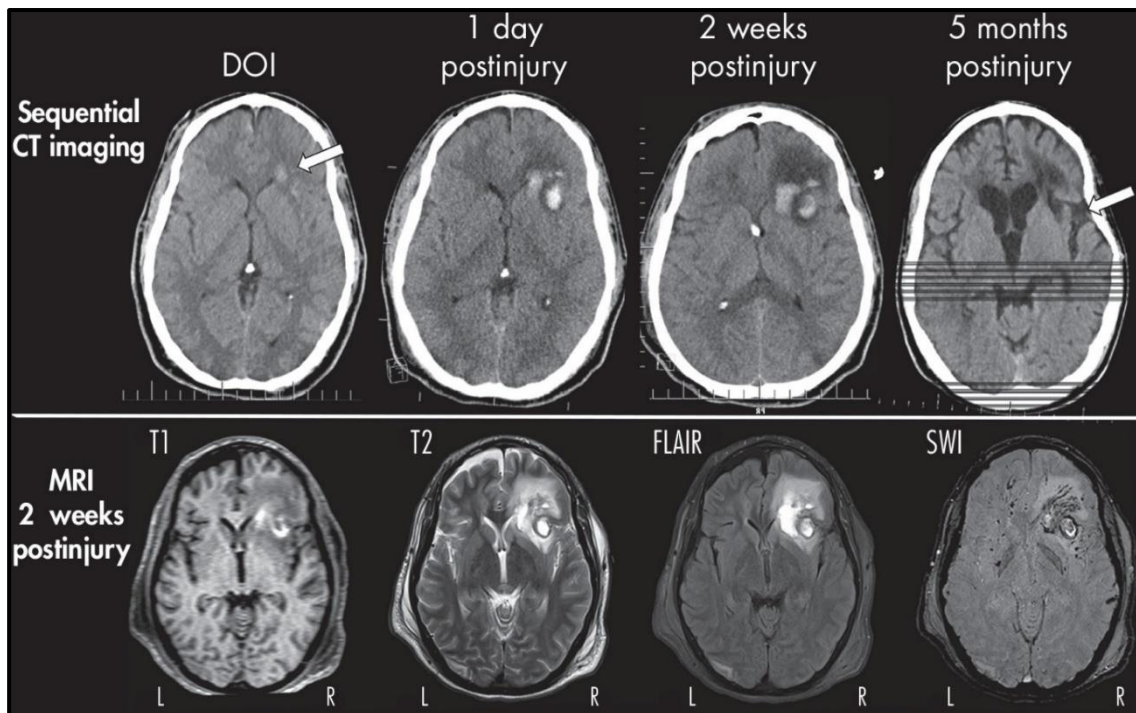


Figure 6. Hemorrhage following TBI. Top Panel: sequential computed tomography (CT) imaging of the evolution of hemorrhage (first white arrow) from day of injury (DOI) to 5 months post-injury. Extensive volume loss has occurred, associated with generalized atrophy, ventricular expansion, and reduced density in deep white matter (last white arrow pointing to the prominent Sylvian fissure). **Bottom Panel:** magnetic resonance imaging (MRI) studies at 2 weeks post-injury showing. The hypo-intense (dark) signal in the susceptibility-weighted imaging (SWI) sequence reflects hemosiderin and where hemorrhagic shear lesions occurred. The fluid-attenuated inversion recovery (FLAIR) sequence highlights the degree of inflammation and beginnings of white matter degradation in the frontal area. (Figure adapted from Wilde et al. [107]).

b. Other Risk Factors

Early seizures are a consistent risk factor of PTE proved by both retrospective and prospective clinical studies [108-110, 116, 117]. Patients with early seizures will go on to have another one in the following two years in 86% of the cases [118]. Similarly, in animal research, they are reported to occur in animals that go on to develop late

spontaneous seizures (PTE) [119, 120]. In addition, skull fractures and dura penetration are also frequently associated with PTE [121]. A retrospective population-based cohort study of more than 19000 TBI cases found that patients with skull fractures have the highest hazard ratio (HR=10.6) for developing PTE [122]. Skull fractures combined with temporal lobe injury and early seizures are the most predictive factors of PTE development [116].

C. Modeling PTE Using TBI Rodent Models

Research aiming at preventing and treating PTE highly relies on identifying the mechanisms by which epileptogenesis occurs. Although studying epileptogenesis in PTE seems easy to approach as the timing of the insult is well known, reproducing PTE in animal models has been challenging. Multiple established models of TBI have been used in an attempt to mimic PTE, with varying degree of success, including the drop weight model, the blast injury model, the fluid percussion injury model (FPI) and the controlled cortical impact model (CCI). In general, the FPI and CCI are the most widely used to study PTE.

1. TBI Animal Models

a. The Fluid Percussion Injury (FPI)

The FPI model is based on the work of Dixon and McIntosh [123, 124], and it involves a central or a lateral craniotomy and exposure of the dura to implant an adapter that transduces energy. Injury is focused on the dura and is induced by an energy wave that propagates along a fluid column. FPI allows the adjustment of the severity of the

injury by manipulating the intensity of the pressure pulse. FPI can produce deformation and displacement of brain tissue, intracranial hemorrhage, and tissue damage at the cortical and subcortical levels [125]. FPI also replicates behavioral changes such as movement coordination deficits and memory impairments [126, 127]. Some disadvantages of this model are the high mortality rate that is possibly due to the unavoidable high degree of severity necessary to develop PTE [128] and the resulting post-injury apnea [129]. Moreover, the sham injury itself has been reported to cause significant damage [130], and even the slightest shifts in the craniotomy placement can dramatically affect behavioral and physiological outcomes [131, 132].

b. The Controlled Cortical Impact (CCI)

First described by Lighthall in 1988 [133], the CCI model involves the use of a computer-controlled pneumatic or electromagnetic impact device to stereotaxically strike the dura following a craniotomy (open-head injury) or the skull (closed-head injury). This model allows better regulation of the injury parameters, by choosing the shape and size of the induction tip, and by controlling the impact's depth, velocity, and duration (dweller time). Injury severity is aggravated by mainly increasing the depth, but there is still no consensus regarding the injury parameters or pathological endpoints to classify the injury's severity in this model. The CCI model can mimic concussion, tissue loss, subdural hematoma, axonal injury, and blood-brain barrier disruption, along with behavioral and cognitive deficits [127]. Open-head injury using the CCI model is almost completely focal, unlike the mixed focal/diffuse injury following FPI, and therefore, a less severe injury is enough to produce cortical damage necessary for epileptogenesis. CCI protocol can also be modified to eliminate the craniotomy and

mimic a closed-head injury, especially relevant in the study of concussion and mild TBI. Nevertheless, most PTE studies using CCI model relies on the open-head model (Table 2).

2. Challenges in PTE Modeling and Available Studies

While TBI animal models do mimic main aspects of TBI pathophysiology and functional deficits, they cannot entirely replicate the human condition. Each model has its limitations and some aspects that still need to be empirically validated. Even anesthesia prior to TBI induction experimental models can have confounding effects. Recently, many efforts have been put into mimicking PTE using TBI animal models. This growing field proved to have its challenges that have prevented the establishment of a platform to study preventive treatments for PTE. Many factors could be hindering experimental PTE research, such as (i) the variability in injury parameters used, (ii) the late latency and low frequency of PTE emergence in rodents, (iii) the lack of a clear definition and characterization of rodents normal and abnormal EEG (Table 1), and (iv) the technical difficulties of long-term EEG monitoring.

On the first hand, and given the high risk of PTE development following open-head injuries, most pre-clinical studies of PTE currently consist of TBI induction following open-head injury, whether using the FPI or the CCI models (Tables 2-4). Fewer attempts are made to study PTE following closed-head injuries [134, 135], although CHI represents the majority of clinical TBI cases and can also lead to PTE, especially in the pediatric population. The craniotomy in and of itself can be a confounding factor since it can prevent normal brain development in juvenile rats. This

can explain why epileptiform discharges and late seizures are sometimes found in sham-manipulated controls [120, 136, 137]. Furthermore, and regardless of the TBI model and injury parameters used, a low percentage of injured rats go on to develop PTE. Even then, the latency period for PTE emergence is considerably long and could be up to a year (Tables 2-4). While this replicates the characteristics of human PTE, it can obstruct animal research given the need for long-term EEG monitoring that could be costly and susceptible to many technical problems. These challenges are further accentuated by the lack of a clear definition of normal rodent EEG, and thus, the variability of PTE percentage can be partially attributed to the different definitions and seizure cutoff duration adopted by the investigators.

Tables 1-4 highlight the methodological differences (rodent strain, age, injury parameters), the differences in seizure definition, and the resulting variability in PTE outcomes.

	Reference	Electrographic definition	Seizure duration cutoff
CCI Model	Kelly et al. 2015 [136]	n.d.	n.d.
	Guo et al. 2013 [138]	identifiable discrete epochs of repetitive spike discharges that evolve in amplitude	≥ 10 s
	Bolkvadze and Pitkanen 2012 [139]	high-amplitude rhythmic discharge that clearly represented a new pattern of tracing (repetitive spikes, SWD, and slow waves)	> 5 s
	Hunt et al. 2009 [140]	n.d.	n.d.
	Statler et al. 2009 [141]	repetitive spiking that persists confirmed by motor seizure	> 15 s
FPI Model	Smith et al. 2018 [137]	N/A	n.d.
	Bragin et al. 2016 [119]	ictal EEG activity lasting with or without behavioral correlates	> 10 s
	Reid et al. 2016 [120]	electrographic event ≥ 10 s with a buildup of rhythmic activity with evolution in at least two of location, amplitude, or frequency, and accompanying change in behavior	≥ 10 s
	Rodgers et al. 2015 [142]	differentiated from background noise by the appearance of large-amplitude, high frequency activity, with progression of the spike frequency	≥ 20 s
	Shultz et al. 2013 [143]	high-amplitude, rhythmic discharges (repetitive spikes, SWD, and slow waves), lasting and showed an evolution in the dominant frequency	≥ 5 s
	D'Ambrosio et al. 2004, 2009, 2011 [144-146]	Epileptiform pattern	≥ 1 s
	Kharatishvili et al. 2006, 2007 [128, 147]	Epileptiform discharges	≥ 5 s
Other Models	Bugay et al. 2019 [135]	n.d.	n.d.
	Shandra et al. 2019 [134]	high-amplitude rhythmic discharges (spikes, polyspikes, SWD, slow waves) with an evolution of the ictal event in amplitude and frequency	≥ 10 s
	Kendirli et al. 2014 [148]	progressive build up in amplitude of rhythmic theta activity or spiking that evolved in frequency to clonic activity followed by a postictal suppression or an initial spike followed by attenuation of amplitude and a subsequent buildup of rhythmic activity	n.d.

Table 1. Different electrographic definitions and seizure duration cutoff in rodent PTE studies. Different seizure definitions are used in PTE studies that relies on TBI rodent models. The variability in the cutoff period (as short as 1s and as long as 20s) can affect the reported percentage of PTE emergence (Tables 2-4). **N/A**= Not Applicable; **n.d.** = not determined.

Reference	Animals	Injury	Mortality, Exclusion	EEG Recording	Duration cutoff	PTE emergence	PTE Seizures				
							Characteristics	Latency (Post-TBI)	Duration	Frequency	Epileptiform Features
Kelly et al. 2015 [136]	Adult male SD rats	Open CCI	43/156 (28%) excluded 4/128 (5%) died	Video-EEG, starting one week post-TBI, for 8-619 days	n.d.	26/128 (20%)	17/88 (19%) Convulsive Class 3-5 (Video proven only)	196.41 ± 33.99 days	87.24 ± 7.53 s	n.d.	SWD in shams and TBI
							7/40 (17.5%) Non-convulsive	80.57 ± 15.95 days	31.89 ± 3.21 s	n.d.	
							2/40 (5%) Class 5 convulsive	162 and 349 days	91.00 ± 12.34 s	n.d.	
Guo et al. 2013 [138]	Adult male CD-1 mice	Open CCI	0%	Video-EEG for 16 weeks post-TBI	≥ 10 s	8/16 (50%)	behavioral arrest, clonic movements of the limbs, rearing and falling over	82.3 ± 10.2 days	35.5 ± 2.8 s	0.27 ± 0.11 seizures per day	Interictal epileptiform spike discharges were relatively rare and tended to be seen on the days of seizure clusters
Bolkvadze and Pitkanen 2012 [139]	Adult male 57BL/6S mice	Open CCI	4/50 (10%)	Video-EEG 6 months post-TBI for 2 weeks	≥ 5 s	4/45 (9%)	Racine 2-5	6 months	50 ± 14 s	0.23 ± 0.11 seizures per day	Epileptiform spiking in 37/45 (82%) in TBI only.
Hunt et al. 2009 [140]	Adult male CD-1 mice	Open CCI	0/34 (0%)	N/A Observation started 42-71 days post injury	n.d.	6/21 (28%)	2/10 (20%) mild TBI, Racine 2	65.70 ± 5.8 days	≥ 90 s	n.d.	N/A
							4/11 (36%) severe TBI, Racine 2-3	61.18 ± 8.55 days			
Statler et al. 2009 [141]	P19 male and female SD rats	Open CCI	2/10 (10%)	Video-EEG Starts 5-8 months post-TBI for 3 months	≥ 15 s	1/8 (13%)	Racine 4-5	260 days	45 – 60 s	4 seizures	EEG spiking in 87.5% of TBI rats on 4-12% of monitored days

Table 2. PTE studies using the CCI rodent TBI model. Summary of PTE results reported using the CCI model in rodents. Only late spontaneous unprovoked seizures are included in this table (excluding early seizures and PTZ-induced seizures). **Note:** **SD**= Sprague-Dawley; **Open CCI**= craniotomy followed by Controlled Cortical Impact; **SWD**= Spike-Wave Discharges; **N/A**= Not Applicable; **n.d.** = not determined.

Reference	Animals	Injury	Mortality, Exclusion	EEG Recording	Duration cutoff	PTE emergence	PTE Seizures				Epileptiform Features
							Characteristics	Latency (Post-TBI)	Duration	Frequency	
Smith et al. 2018 [137]	Adult male Wistar rats	Lateral FPI (Severe)	45% died	N/A Video + Accelerometer	n.d.	5/8 (62.5%)	Racine 4-5	2 - 5 weeks	n.d.	2-5 seizures per rat	SWD in shams but more in TBI
Bragin et al. 2016 [119]	Adult male SD rats	Lateral FPI	6/18 (34%) died	Video-EEG Immediately post-TBI for 28-189 days	> 10 s	4/12 (30%)	Generalized SE. All died following SE	8-24 weeks	8-10 hours	1-6 seizures per hour	pHFOs and rHFOS in TBI only
Reid et al. 2016 [120]	Adult male SD rats	Lateral FPI (different severities)	4/34 died 2/30 excluded	Video-EEG (intermittent) immediately and up to 26 weeks post-TBI	≥ 10 s	Focal: 14/28 (50%) and 1/7 (14%) sham or Generalized: 3/28 (11%)	Focal with behavioral arrest or Generalized with SE and sustained clonus	8 - 33 weeks	19 - 27 s	4.4-26.4 seizures per week	rHFOS frequency increases with severity and decreases with time
Rodgers et al. 2015 [142]	Adult male SD rats	Rostral parasagittal FPI (moderate and severe)	13/50 with 10% mortality	Video-EEG 2 weeks and up to one year post-TBI	≥ 20 s	0%	N/A	N/A	N/A	N/A	0% had spikes and SWD of same characteristics in both shams and TBI
Shultz et al. 2013 [143]	Adult male Wistar rats	Lateral FPI	11/45 (24%) 1 died and 10 excluded	Video-EEG 6 months post injury for 2 weeks	≥ 5 s	7/23 (30%)	n.d.	6 - 7 months	52.9 s	6.2 seizures in the 2 weeks of recording	12/23 (52%) with epileptic discharges (mean number 11.5) in TBI only
Bolkvadze and Pitkanen 2012 [139]	Adult male CD-1 mice	Lateral FPI	9/45 (20%)	Video-EEG 6 months post-TBI for 2 weeks	≥ 5 s	1/31 (3%)	Racine 2	6 months	91 s	1 seizure	22/31 (71%) in TBI only
D'Ambrosio et al. 2004^a, 2009^a, 2011^{a,b} [144-146]	P32-35 male SD rats	Rostral ^a or medial ^b parasagittal FPI	9/89 8% ^b -11% ^a	Video-EEG Weekly 24 hours, up to 5.4 ^b - 7 ^a months post-TBI	≥ 1 s	100%	No behavioral changes or motor arrest with or without automatisms	2 - 19 weeks	1-99 s ^a 1-35 s ^b	0.2-0.6 ^b and 3-5 ^a seizures per hour	n.d.
Kharatishvili et al. 2006^c, 2007^d [128, 147]	Adult male SD rats	Medial parasagittal FPI (Moderate)	25% ^d - 33% ^c out of n= 64 ^c	Video-EEG starting 7-9 weeks post-TBI and up to 12 months post-TBI	≥ 5 s	0% ^d 43% - 50% ^c	Racine 2.3 - 3.3 Partial and/or (secondary) generalized	4 - 11 weeks	113 ± 46s ^c	0.3 ± 0.2 seizures per day	80% ^d , in TBI only

Table 3. PTE studies using the FPI rodent TBI model. Summary of PTE results reported using the FPI model in rodents. Spontaneous late seizures had generally a long and variable latency period, and TBI/PTE characteristics varied between the studies. **Note:** SD= Sprague-Dawley; FPI= Fluid Percussion Injury; SWD= Spike-Wave Discharges; pHFOs: pathological High Frequency Oscillations; rHFOS= repetitive HFOs and Spikes; SE= Status Epilepticus; N/A= Not Applicable; n.d. = not determined.

Reference	Animals	Injury	Mortality, Exclusion	EEG Recording	Duration cutoff	PTE emergence	PTE Seizures				Epileptiform Features
							Characteristics	Latency (Post-TBI)	Duration	Frequency	
Shandra et al. 2019 [134]	Adult male and female C57BL/6 or Aldh1l1-eGFP//FVB/N mice	Repetitive mild Weight-drop	(2-7%)	Continuous, 5-7 days post injury for 110 days	≥ 10 s	4/9 (44%)	3/9 (33%) convulsive 1/9 (11%) non-convulsive	38 ± 7.642 days	> 10 s	0.3 seizures per day	n.d.
Bugay et al. 2019 [135]	Adult male C57BL/6J mice	Repetitive mild blast injury	n.d.	Monthly intervals of 72 hours for 10 months Video-EEG	n.d.	6/13 (46%)	Non-convulsive	8 weeks – 10 months	38.8 ± 3.9 seconds	2.2 ± 0.4 seizures in total	n.d.
Kendrili et al. 2014 [148]	Adult male SD rats	Penetrating copper wire	5/31 died 3/26 excluded	Starts 6 months post-TBI until 11 month (intermediate)	n.d.	22/23 (96%)	Racine 4	n.d.	33.8 ± 2.6 s	3.6 ± 0.34 Seizure per day	n.d.
		Penetrating steel wire	3/17 died 1/14 excluded			0/7 (0%)	N/A	N/A	N/A		
		Lesion only	0/7 (0%)			3/13 (23%)	Racine 1	n.d.	25.7 ± 0.7 s	0.2 ± 0.06 seizure per day	

Table 4. PTE studies using different TBI models. Summary of PTE results reported using different models of TBI in rodents. **SD**= Sprague Dawley; **N/A**= Not Applicable; **n.d.** = not determined.

D. Differences in the Coagulation Profile Between Humans and Rats

It is important to always consider the cross-species differences when using animal models. While rats are a widely used animal species in many TBI and PTE studies, some species differences can be probably hindering a more optimal replication of human conditions. Here we focus on the differences in bleeding/coagulation in humans and rats, given the importance of hemorrhage in injury mechanisms and its high correlation with PTE emergence. In general, rats' blood is more prone to coagulation than humans, thus less prone to bleeding. First, the clotting time in rats is three-folds shorter than humans (207 seconds vs. 595 seconds), and the thrombin dose required to shorten this time is 100-fold higher in rats (0.2 IU vs. 0.002 IU). Furthermore, rats have 6-fold higher platelets count (1180 G/L) than in humans (187 G/L) [9]. Direct inhibition of the coagulation factor Xa with DX-9065x also requires 40-fold higher dose in rats [149]. These difference, among others, in the coagulation profile is a limitation in blood-related studies that rely on rat models.

In general, using animal models to study human diseases always have its limitation, since ultimately the best models of human conditions are humans. It may be impossible for a single model to reproduce all features and comorbidities of TBI, especially given the preexistent differences that might be affecting outcomes. For that, certain criteria can help assess the validity of the model, depending on the scientific question and the sought outcomes. Hence, an animal model of PTE can be discussed in terms of construct, face, and predictive validities, first described by Willner for animal models of depression [150]. Construct validity refers to the similarity of etiology and the underlying mechanisms of a disease between animals and humans. Face validity is

measured by how much a model mimics human disease phenotype (symptoms and signs), and the PTE model should have electrophysiological behavioral, and histopathological similarities to the human. Predictive validity is how well a model can predict the unknown aspects of a given human disease (e.g., treatments outcomes). Animal models may be predominately based on one of these validity aspects, while others tend to sacrifice one of these criteria to better reinforce the others. The appropriateness of using a model in a research study is a function of the scientific question and the sought outcomes, whether it is designed to study mechanisms, symptoms, or treatments.

CHAPTER II

AIMS AND HYPOTHESES

A major obstacle in gaining new insights into the condition of PTE is the lack of well-established animal models. Available studies mainly rely on the open-head models of TBI and have had variable degrees of success in inducing PTE. However, closed-head injuries and ensuing PTE also entail investigation given that closed-head injuries are far more common than open-head injuries, especially in the pediatric population. Therefore, we propose to validate a peri-adolescent rat model of closed-head injury, while also focusing on hemorrhage being an important risk factor of PTE. We hypothesize that chemically promoting substantial hemorrhage following impact will increase the risk of PTE emergence. Rats are relatively less prone to bleeding compared to humans, and one way to bypass the aforementioned differences in the coagulation profiles (Section I-D) is by using an anti-coagulation agent. In this study, rats are injected with a pre-impact heparin dose, a widely used anti-thrombin dependent anticoagulant, in order to promote bleeding and increase the risk of PTE emergence. The partial sacrifice of construct validity (the use of heparin) aims to improve the face validity of the model (increased PTE risk). The use of chemicals is not uncommon in epilepsy translational research, and the most commonly used animal models depend on chemically-inducing seizures with chemoconvulsants (e.g., kainic acid or pilocarpine).

Closed-head TBI will be induced using the modified controlled cortical impact model. Following impact, rats will be subjected to long-term EEG monitoring and behavioral testing, then sacrificed for histological analyses.

Aim 1: To investigate the reproducibility and efficacy of inducing a closed-head traumatic brain injury with prominent hemorrhage in peri-adolescent Sprague-Dawley rats, and to study its long-term effect on the emergence of epileptiform features and spontaneous seizures (long-term EEG recording for up to 3 months post-TBI).

Hypothesis 1: The administration of an anticoagulant (heparin) prior to closed-head TBI induction will lead to substantial hemorrhage, and the subsequent injury will lead to higher rates of epileptiform features and spontaneous seizures.

Aim 2: To investigate the effect of hemorrhagic closed-head TBI on the emergence of long-term cognitive behavioral deficits (6 weeks post-TBI).

Hypothesis 2: Injured rats with more prominent hemorrhage and epileptiform features will display deficits in hippocampal-dependent visuospatial navigation and learning (Morris water maze and active avoidance tests).

Aim 3: To assess the histopathological changes following hemorrhagic closed-head TBI.

Hypothesis 3: Heparinized TBI rats will have higher levels of hippocampal and cortical GFAP (48 hours post-TBI), along with lower hippocampal and cortical neuronal densities (3 months post-TBI) compared to the non-heparinized TBI rats and compared to controls. The damage caused by the hemorrhagic closed-head TBI will correlate with the observed epileptiform features and cognitive deficits.

CHAPTER III

MATERIALS AND METHODS

A. Animals and Experimental Design

All experiments were approved by the Institutional Animal Care and Use Committee (IACUC) at the American University of Beirut. Forty-three male Sprague-Dawley rats were housed in a temperature-controlled room and maintained on a 12-hour light-dark cycle with ad libitum access to food and water. At peri-adolescent age (P35), rats were subjected to a single-hit closed-head traumatic brain injury or were sham manipulated. Following TBI, rats underwent epidural electrodes implantation surgery and long-term continuous EEG recording, starting 2 weeks post-injury (P50), until 3 months post-injury (P130). EEG was interrupted between P80 and P100 for behavioral testing. Histological analyses included immunohistochemistry to assess the glial fibrillary acidic protein (GFAP) levels and neuronal density (NeuN) at P37 and P130, respectively.

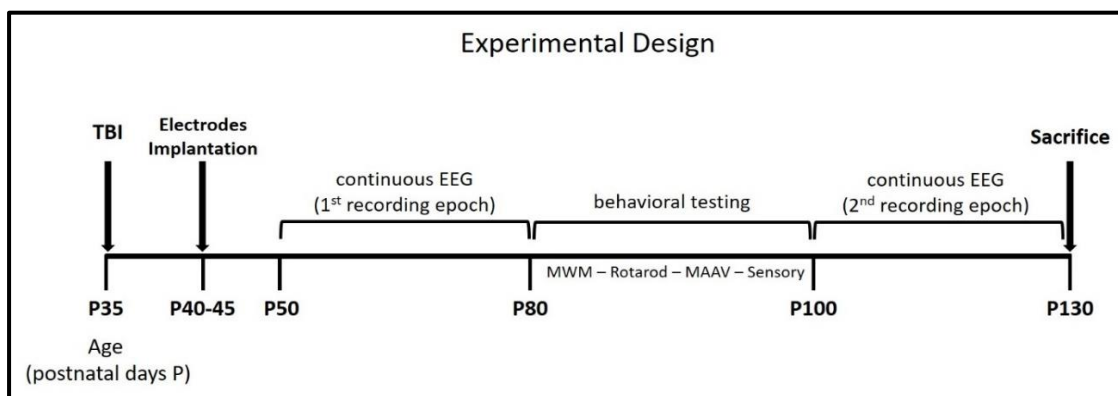


Figure 7. Experimental design of the project. Following TBI at P35 and a post-injury resting period, rats underwent electrodes implantation surgery between P40 and P45. After a post-operative resting period, long-term continuous EEG recording was obtained for one month between P50 and P80. This was followed by behavioral testing paradigms including the Morris water maze (MWM), the Rotarod motor test, the modified active avoidance (MAAV), and the Von Frey and Hargreaves sensory tests. EEG recording was continued for another continuous month between P100 and P130, where rats were sacrificed for histological analyses. A subgroup of rats was sacrificed at P37 for early histological assessment, 48 hours post-injury (not illustrated in this figure).

B. Closed-Head Traumatic Brain Injury Induction

TBI was induced in male Sprague-Dawley rats at peri-adolescent age (P35) using the controlled cortical impact injury protocol. Rats were anesthetized using an anesthetic cocktail, administered intramuscularly, containing a combination of ketamine (60mg/Kg), xylazine (6mg/Kg) and acepromazine (1.25mg/Kg). Once appropriate anesthesia was achieved (lack of response to toe-pinching), rats received a single intraperitoneal injection of heparin (600 IU/Kg) or a volume matched injection of normal saline (0.9% solution). Rats were divided into the following 4 groups:

1. **NS group:** sham manipulation after normal saline injection (n=10)
2. **HP group:** sham manipulation after heparin injection (n=8)
3. **CTBINS group:** Closed-TBI induction after normal saline injection (n=14)
4. **CTBIHP group:** Closed-TBI induction after heparin injection (n=11)

TBI or sham manipulation was done 20 minutes following heparin or normal saline injections. The rat was placed on a stereotaxic frame and, its head was firmly secured using two ear bars. A sterile ophthalmic ointment was applied on each eye to protect it from drying out. Using aseptic techniques, a midline scalp incision was made and the skin overlying the skull was retracted. The impact was targeted over the right parieto-temporal region of the skull using a controlled stereotaxic impactor device (ImpactOne™ Stereotaxic impactor for CCI, Leica Biosystems Inc., Germany). The injury was induced using a 5 mm flat plastic tip affixed to a pneumatic impactor with an impact duration of 1 sec, a depth of 1.5 mm, and a speed of 6.5 m/sec. The injury site was then sutured, and antibiotic ointment was applied. The rat was then placed on a heat-pad and monitored until the regain of wakefulness and normal activity. After the procedure, the rats were transferred to their respective cages, and an analgesic regimen

with paracetamol (1mg/ml) was administered for 3 days. Rats were given a resting period of 5-7 days before undergoing EEG electrodes implantation surgery.

C. Surgical EEG Electrodes Implantation and EEG Recordings

Epidural electrodes implantation surgery was performed as previously described between P40 and P45 (Figure 8) [151, 152]. The same anesthetic cocktail (ketamine, Xylazine, and acepromazine) was administered intramuscularly. Once the response to toe pinching disappeared, the rat was placed on a pad, and the hair was shaved with a trimmer from the flat of the nose between the eyes down to the neck. The rat's head was then secured on a stereotaxic frame with two ear bars. Eyes were protected from irritation by applying a lubricating eye ointment. The scalp is then sterilized with 10% iodine solution and 70% ethanol. A 2 cm midline incision is made, and the skull was exposed using a retractor. After cleaning and drying of the calvarium's surface, five 1.4 mm holes were made using a high-speed driller. Five epidural screw electrodes were then placed (1.6mm in diameter and 4.5mm in length) including two frontal electrodes (left: F3 and right: F4) were placed 2mm anterior and 3mm lateral to the bregma, and two parietal (left: P3 and right: P4) were placed 5mm posterior and 3mm lateral to the bregma. One anterior midline electrode (6 mm anterior to the bregma) was used as a reference. The positions of these electrodes were determined based on the Sherwood and Timiras Atlas of the developing rat brain. A plastic-sheathed wire with an exposed uninsulated tip was used as a ground electrode and was placed under the skin. The electrode wires and the ground wire were then inserted in a 6-channel pedestal (MS363, Plastics One, USA). Acrylic dental cement was then used to cover the electrodes and the pedestal, giving the final shape to the "headset". Neomycin was applied to prevent

postoperative infections. After the surgery, the rats were transferred to customized single-animal EEG cages, and an analgesic regimen with paracetamol (1mg/ml) was administered for 3 days.

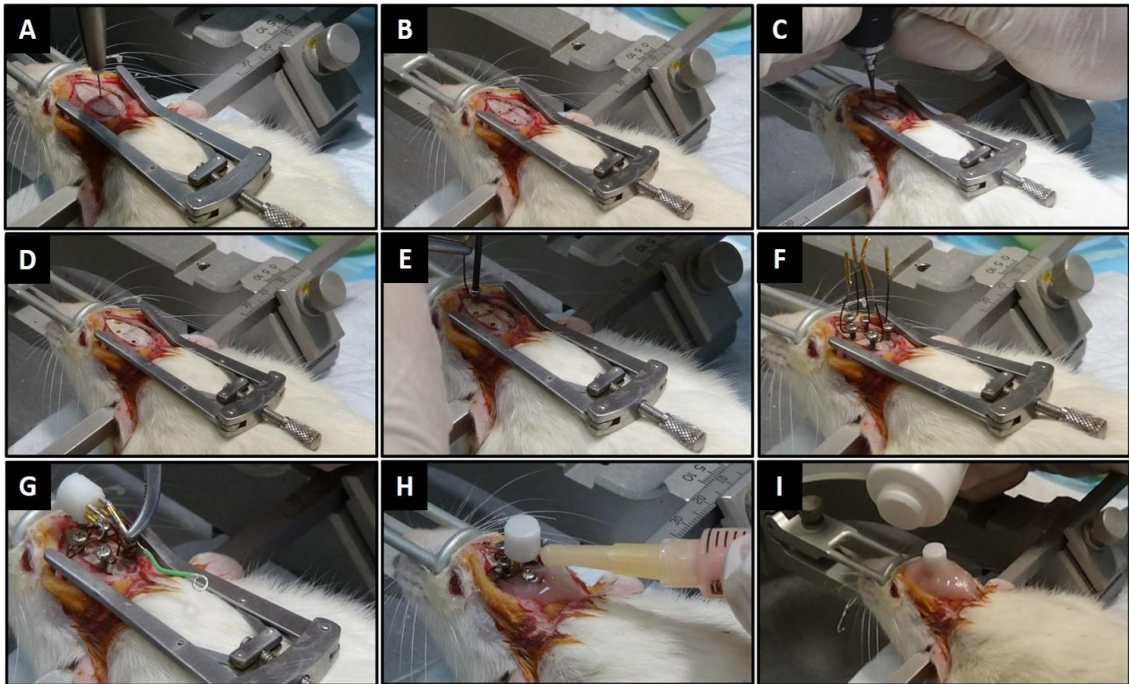


Figure 8. Electrodes implantation surgery. **Panel A:** Identification of the antero-posterior and the lateral coordinates of the bregma with the stereotaxic arm. **Panel B:** Marking of the drilling holes of the electrodes by moving the stereotaxic arms to the calculated coordinates (according to bregma). **Panels C and D:** Drilling of five small holes with a high-speed drill held in the vertical position above the skull's surface. **Panel E:** Insertion of the screw electrodes using a screw driver. **Panel F:** The two frontal and two parietal electrodes, along with one reference electrode. **Panel G:** Insertion of the wires' sockets in the 6 channels pedestal. **Panel H:** Pouring of acrylic dental cement to fill the entire incision site. **Panel I:** Application of antibiotics to the final headset.

Following a post-surgical resting period, rats were attached to the customized EEG system [151, 152] (Figure 9), and long-term continuous EEG recording was initiated. EEG monitoring started 2 weeks post-TBI for one month (P50-P80, first recording epoch). After the completion of the behavioral tests, EEG was obtained for another continuous month (P100-130, second recording epoch) (Figure 10). All EEG files were reviewed by two observers blinded to the groups' experimental conditions. EEG was screened for seizures and abnormal electric features. Quantification of electric

features was done daily in 8 sampled hours during the first epoch of recording, and in 4 sampled hours (alternated days) in the second epoch of recording (Figure 10).

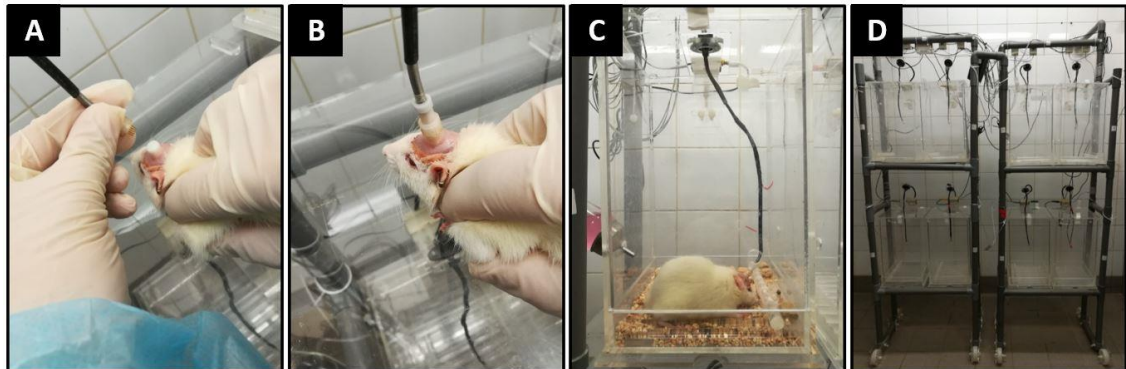


Figure 9. Initiating of EEG recordings. Panels A and B: the rat's headset is attached to the EEG cable. Panel C: Rats are placed in special cages equipped with a swivel-balance commutator that accommodates all sorts of the rat movements in both the horizontal and vertical planes. Panel D: the full EEG rack setup housing 8 cages built with non-conductive material in order to electrically shield the rats from each other and from external electrical sources, and thus providing high quality (high signal to noise ratio) EEG recording.

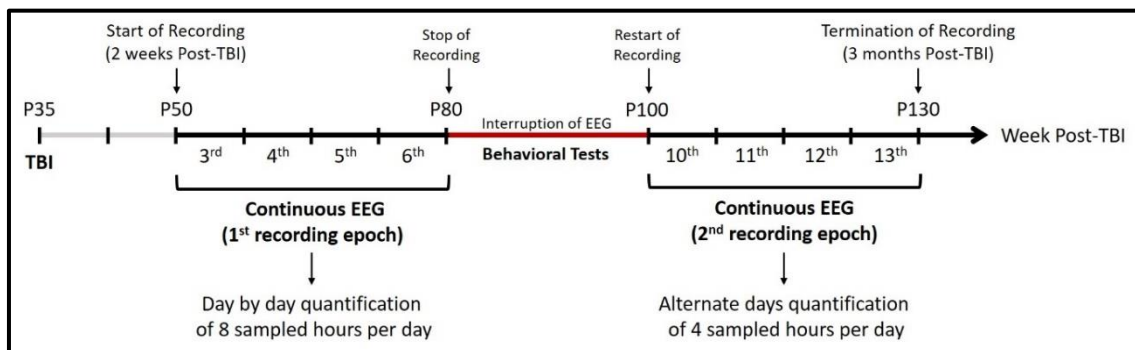


Figure 10. EEG recording epochs. Recording started two-weeks post-TBI for one continuous month until the start of the behavioral tests (first recording epoch, P50-80). EEG recordings were then obtained for another continuous month (second recording epoch, P100-P130). EEGs were screened for seizures, and epileptiform features (spikes and polyspikes) were quantified daily in 8 sampled hours during the first epoch of recording, and quantified in 4 sampled hours (alternate days) during the second epoch of recording.

D. Behavioral Panel

Rats belonging to all four groups described above underwent cognitive behavioral tests, in addition to motor and sensory tests. Rats were first subjected to the

Morris water maze at P80 (6 weeks post-injury), followed by the Rotarod motor test, the modified active avoidance test, and finally to the Von Frey and Hargreaves sensory tests.

1. Morris Water Maze (MWM)

This test consists of habituation and 3 subsets performed over 6 days [153]. A dark-blue circular plastic pool (Coulbourn Instruments, USA), 150 cm in diameter and 80 cm in height, was filled to a depth of 30 cm with water (26°C). The pool is virtually divided into 4 quadrants (Figure 11). During habituation, rats were allowed to swim freely for 2 minutes without an escape platform. During the spatial acquisition phase (Days 1-5), a submerged “invisible” escape platform (transparent plexiglass cylinder) was placed 2 cm below the water surface and remained in the same position during all training days. The rat underwent four daily trials, and was placed in four different immersion landmarks in the quadrant opposite to that of the escape platform. If the rat failed to find the escape platform in two minutes, it was placed on it for 30 seconds by the operator. On day 6, the platform is removed, and the rat was placed in a novel immersion point, opposite to the previous platform location, and was allowed to swim freely for two minutes in order to assess the retention of spatial navigation. Following the probe trial, motor and visual functions were assessed by placing a visible platform (white opaque plastic cylinder) with 4 trials using 4 different immersion points. All MWM experiments were video recorded, and the automated SMART tracking software was used to measure the escape latencies (defined as the time required to escape from the water and reach the platform), as well as the time spent in the probe quadrant in the probe trial.

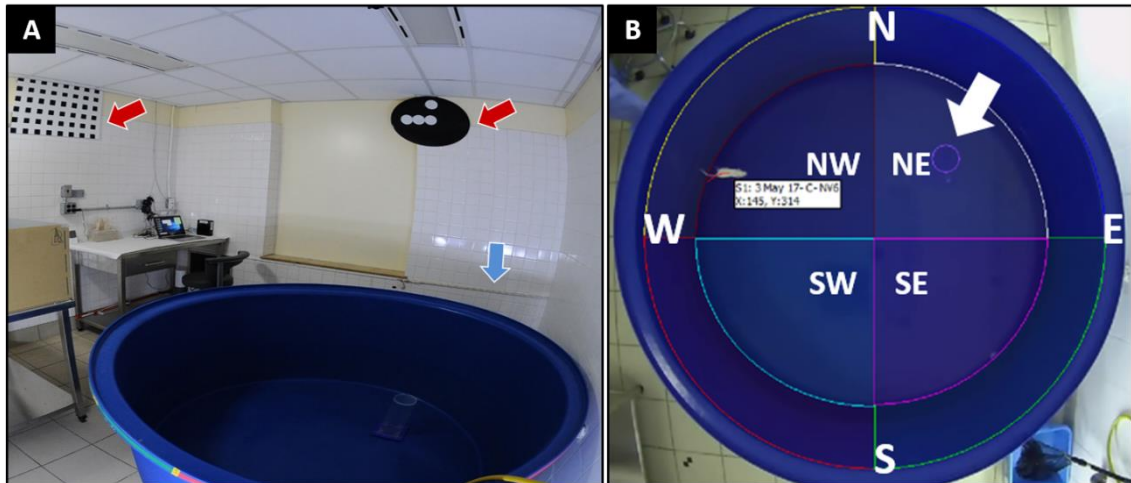


Figure 11. Morris water maze. **Panel A:** The circular dark blue pool is placed in a fixed position in the room and surrounded by 3 distal visual cues, 2 of which are shown (red arrows). Horizontal wall LED lights, one of which is shown (blue arrow) are used for homogeneous light distribution. **Panel B:** MWM during the acquisition phase. An invisible platform (white arrow) is placed in the NE quadrant below the water surface, and the rat is placed in the pool over four sessions from four immersion landmarks that were equidistant to the platform and their sequence was changed every day. (NW: north-west; NE: north-east; SW: south-west; SE: south-east).

2. Rotarod

Following the MWM, rats underwent the rotarod test (Rat Rotarod NG, Ugo Basile, Italy) to assess motor coordination and balance. Rats were acclimatized to the testing room for one hour before starting the training test. During the training phase, rats were placed on the rotating beam, facing away from the operator, for one minute at a constant speed of 5 rpm. Following training, the Rotarod test consisted of three trials, with 10 minutes inter-trial resting period, of accelerated speed going from 4 rpm to 40 rpm in 300 seconds. In case the rat passively rotated or fell in less than 5 sec, the trial was restarted. The apparatus was cleaned between trials with an odorless detergent. The latency to fall from the accelerated rod was automatically measured by the rotarod machine.

3. Modified Active Avoidance (MAAV)

This test was developed at our laboratory to simultaneously assess contextual and auditory conditioning, along with adaptive emotional learning [153, 154]. The MAAV shuttle box (Coulbourn Instruments, US) consists of two equal compartments connected via an opening in the middle of the partition wall (Figure 12). The shuttling box is placed in a soundproof isolation cubicle and is equipped with a tone generator and infrared beam sensors to detect transitions between the two compartments. On habitation day (Day 0), the walls of both compartments were covered with white foam panels, and the rat was allowed to roam freely in the box for 5 minutes. During training days (Days 1-6), the left compartment remained unchanged, while the right compartment was visually modified for contextual conditioning (visuals cues and foam wall plates with black-white stripe patterns) (Figure 12). Using the software provided by the Habitest Modular System (Graphic State IV GS4), a protocol was customized so that a 15 sec tone is followed by an incoming foot-shock (0.5 mA, 15 sec duration) in the left chamber (but not in the right one), with a 40 sec inter-trials resting period. Shuttling to the right side prevents the incoming tone-signaled shock (avoidance) or terminate an ongoing one (escape). In the right chamber, an electrical foot-shock is not signaled by an auditory tone; however, it is delivered for every 10 sec spent in that compartment. Shuttling to the left side prevents or terminates the context-cued foot-shock. This cycle is repeated for a total of 30 trials. On day 7, a two-parts retention test is done in order to assess the retention of auditory and contextual learning separately. During the first part (contextual retention test), the rat was allowed to roam freely in the shuttle box for 2 minutes without electric foot-shocks, and the rat's preference to the left chamber (avoiding the right one) was assessed. During the second part (auditory

retention test), both chambers were similar to the habituation day (white wall panels and no visual cues on both sides), and the following protocol was run: following 5 minutes of acclimatization, 30 tone-signal trials were delivered, with a 30 sec inter-trial interval. Shuttling between the compartments prevents (avoidance) or terminates (escape) the tone-signal foot-shock. The shuttle box was cleaned after each rat with odorless detergent and 70% alcohol solution. All sessions were video-recorded, and the GS4 software provided the time spent in each compartment and the percentage of avoidance or escape from the auditory-cued shocks (auditory conditioning) and from the context-cued shocks (contextual conditioning).

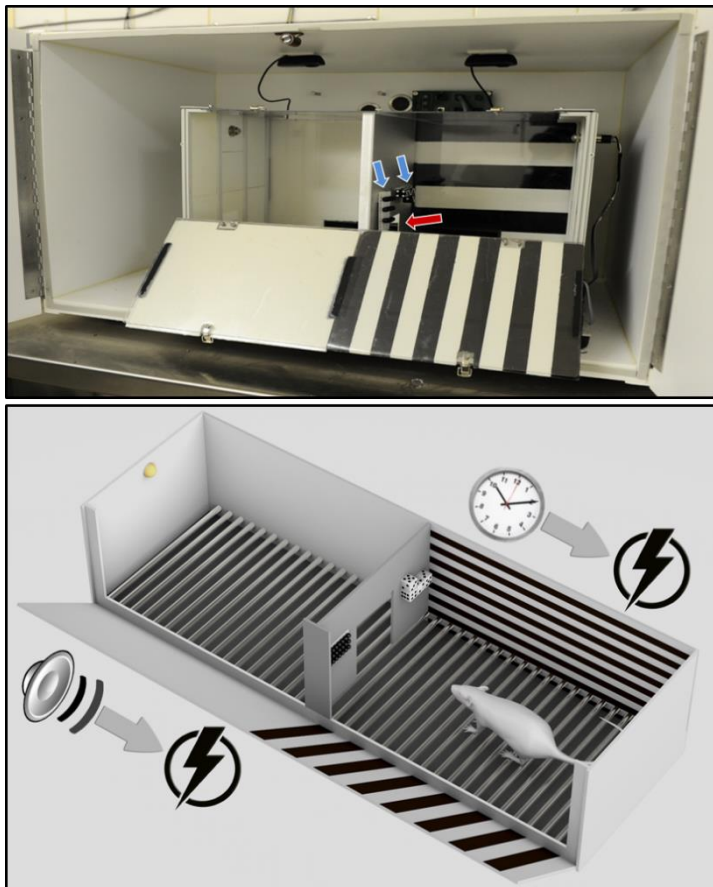


Figure 12. Modified active avoidance. The modified shuttling box is placed in a sound proof cubicle. It consists of two compartments communicating via a door (red arrow) in the middle of a metallic partition wall. The boxes are equipped with a tone generator and infrared beam sensors that monitor rat transitions between compartments. The left compartment is covered with white foam panels whereas the right one is covered with black and white painted foam panels and modified with additional objects fixed on the partition wall (blue arrows). An incoming electrical foot-shock is signaled with a tone in the left chamber, however, it is regularly administered for every 10 sec spent on the right side.

4. Sensory Tests: Von Frey and Hargreaves

The response to mechanical and thermal stimuli was measured by the Von Frey and the Hargreaves tests respectively, on two separate days. Sensory testing was done given that the impact was targeted over the parietal area where the somatosensory cortex is found, was done and in the framework of the MAAV test in order to validate the animals' capacity to sense the electrical foot-shock.

a. Von Frey

Hind paws mechanical sensitivity was evaluated using two Von Frey hair filaments (Aesthesio Semmes-Weinstein monofilaments set, Ugo Basile, Italy) of different forces: the 2g (19.6 mN, non-painful) and the 15g (147 mN, painful). The rat was habituated for 15 minutes in a transparent box on a metal wire mesh floor. The monofilament was applied to the mid-plantar area of both hind paws with a pressure that causes the filament to buckle. Withdrawal or licking of the paw was logged as a positive response. Testing consisted of applying the filament 5 repeated times, for 3 trials with 5 minutes inter-trials interval, starting with the 2g filament.

b. Hargreaves

The Hargreaves test (Hargreaves Apparatus, Ugo Basile, Italy) was used to assess thermal nociception by measuring the latency for hind paws withdrawal in response to a thermal stimulus. The rat was habituated for 15 minutes in a transparent box on top of a glass table. A 40% intensity infrared light was applied to the plantar surface of both hind paws, for 5 trials with 10 minutes inter-trials resting period. A 20 sec cutoff time was set to prevent tissue damage. The latency for hind paw withdrawal was automatically measured by the apparatus.

E. Euthanasia and Cardiac Perfusion Surgery

Following behavioral testing and long-term EEG recording, rats were sacrificed for histological analysis at P130. A subgroup of rats (n=3 for each group) was sacrificed 48 hours post-TBI at P37 for early histological studies and therefore did not undergo the long-term experimental paradigm.

After general anesthesia (same anesthetic regimen used during TBI and EEG surgeries), an abdominal incision is made just below the diaphragm. The heart was then exposed by removing the diaphragm and making two vertical cuts in the rib cage in order to lift it. A needle was then inserted into the left ventricle, and the right atrium was cut to allow the drainage of blood and fluids. PBS was slowly pumped through the inserted needle until all the blood has been flushed out. The brain was then perfused with 4% paraformaldehyde (PFA) in phosphate-buffered saline (PBS) (pH=7.4). Following extraction, the brain was kept in 4% PFA for one day. The brain was then embedded in paraffin and cut into 8 μ m coronal sections for histological and immunohistochemistry analyses.

F. Immunohistochemistry for GFAP and NeuN

Sections for Immunohistochemical (IHC) staining were selected by visual inspection so that their structural patterns match the coronal sections located 2.4 – 2.7 mm posterior to bregma according to the Sherwood and Timiras Atlas of the developing rat brain (for GFAP assessment at P37, 48 hours post-TBI), or located 3.3 – 3.8 mm posterior to bregma based on the Paxinos and Watson adult rat brain atlas (for neuronal density assessment at P130, 3 months post-TBI).

Two sections per brain (n=3 for each group, at both time-points) were analyzed. Same IHC protocol was applied, and the primary antibody used was either anti-GFAP (1:1000 EnCor Biotechnology, USA) or anti-NeuN (1:100 Sigma-Aldrich, Germany). Sections were first deparaffinized with xylene and rehydrated with decreasing concentrations of ethanol. Slides were then incubated in sodium citrate buffer (95°C, pH=6) for antigen retrieval and washed with PBS. Endogenous peroxidase activity was blocked using peroxidase block (Novolink IHC kit, Leica Biosystems, Germany) at room temperature. Following PBS washing, sections were incubated with the primary antibody solution overnight in a humidified chamber at 4°C. During the second day, sections were washed and incubated with horse-radish peroxidase HRP-conjugated secondary antibodies for one hour (sc-516142, Santa Cruz Biotechnology, Texas, USA). After washing, slides were incubated with DAB for revelation and counterstained with 0.1% Hematoxylin.

Images of the sections were taken using the uScope Slide Scanner (Microscopes International, USA). The ImageJ software was used to measure GFAP optical density, and to assess cortical and hippocampal neuronal density by counting NeuN-positive cells. For GFAP, the hippocampus area was defined by outlining its borders along the ventricles. For NeuN, hippocampal neuronal count was done for the CA1-CA3 layers, and in the cortex, a virtual rectangle was drawn directly above the CA1 layer of the hippocampus, and its surface area was automatically provided by the software. Neuronal density (per millimeter squared) was calculated by dividing the total neuronal count onto the surface area.

G. Statistical Analysis

Statistical analyses were performed using Prism 7 (GraphPad Software, USA). One-way analysis of variance (One-way ANOVA) followed by post-hoc Fisher least significance difference LSD test was used to analyze the MWM probe trial (intra-group) and visible platform tests, the rotarod test, the MAAV retention data, the sensory tests, along with the histological data. Two-way ANOVA with repeated measures in conjunction with the post hoc Fisher LSD test was used to analyze the MWM and the MAAV acquisition phases.

CHAPTER IV

RESULTS

A. Closed-head TBI induction with prominent hemorrhage

Closed-head TBI was successfully induced in peri-adolescent rats over the right parieto-temporal skull, using the controlled cortical impact (CCI) model. Immediately after impact, both TBI groups (CTBINS and CTBIHP) showed acute bleeding upon visual inspection of the skull. The heparinized group (CTBIHP) had a more prominent hemorrhage, with visual evidence of contralateral injury (Figure 13-A). All rats survived the procedure with no skull fractures or indentation.

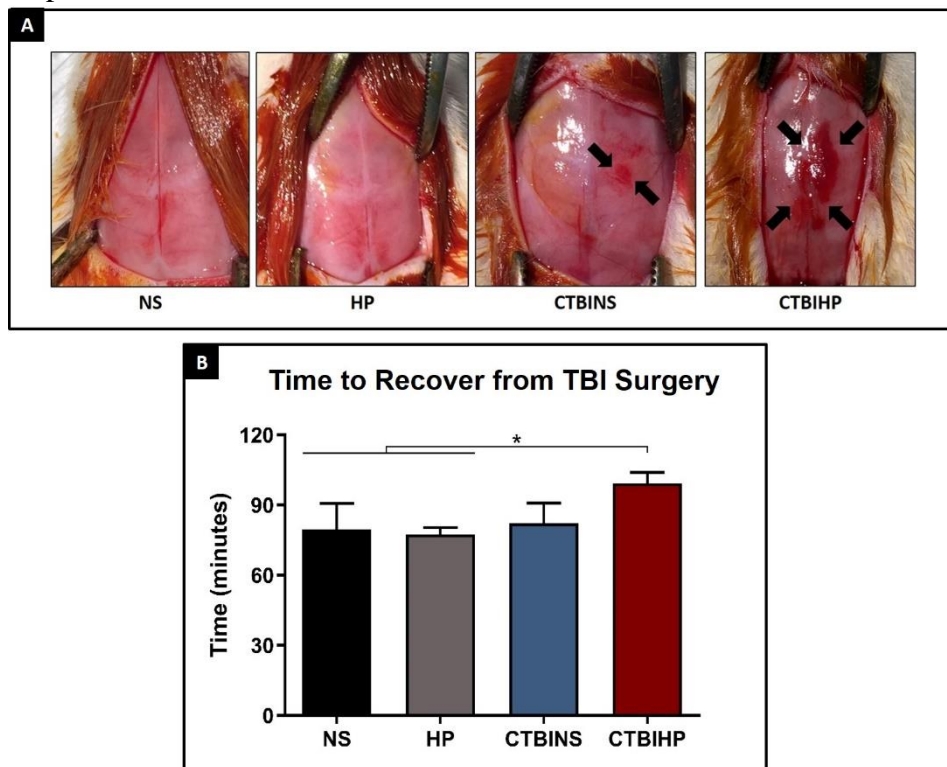


Figure 13. Post-TBI hemorrhage and post-surgery recovery time. **Panel A:** Both TBI groups had a bleeding under the skull after the impact, ipsilateral to the injury site (right side), with the CTBIHP showing a more prominent hemorrhage than the CTBINS. By visual inspection, the CTBIHP had evidence of a contralateral injury. The control groups (NS and HP) showed no bleeding under the skull. **Panel B:** The time between the administration of anesthesia and the regain of wakefulness and ambulation following TBI was measured (NS = 79.5 ± 11.13 min; HP = 77.33 ± 3 min; CTBINS = 82.12 ± 8.7 min; CTBIHP = 99.3 ± 4.6 min). The CTBIHP were significantly slower than the NS and HP controls ($p < 0.05$, One-Way ANOVA with post-hoc Fisher's LSD test). (NS= controls with normal saline n=10; HP= controls with heparin n=8; CTBINS= Closed-TBI with normal saline n=14; CTBIHP= Closed-TBI with heparin n=11). The results are reported as mean ± SEM.

Rats recovered from TBI surgery anesthesia and were fully awake and ambulatory after 78 to 100 minutes (Figure 13-B). Notably, CTBIHP was slower than all groups, and significantly slower when compared to the controls ($p < 0.05$). Moreover, immediately after impact all of the CTBIHP rats, and none from the other groups, showed signs of hypothermia and labored breathing that lasted for a few minutes.

B. EEG findings: increased hyperexcitability after hemorrhagic closed-head TBI

The entire EEG tracings were screened for seizures, spikes, and polyspikes. Their frequency was quantified in daily sampled epochs (Section III-C). EEG reading revealed the emergence of spikes in both TBI groups and more so in the CTBIHP group (as discussed below). Furthermore, even though polyspikes were found in all groups, sampled quantification revealed a considerable increase of polyspikes frequency in TBI groups. No seizures were detected, and all TBI rats had intermitted slowing superimposed over the normal electrical activity.

1. Spikes

Spikes were only detected in both TBI groups and were absent in the control groups. These electrical discharges (duration < 250 milliseconds) were clearly and morphologically distinguishable from the background activity. They had a pointed peak, followed by a repolarization wave (Figure 14). Spikes were prominent in amplitude in, and thus localized to, the ipsilateral side of the injury (right side). During the first week of EEG recording, 2 weeks post-TBI, spikes were significantly more abundant in the heparinized TBI group (48.911 ± 5.623 spikes/hour, $p < 0.05$) compared to the non-heparinized group (16.46 ± 1.867 spikes/hour) (Figure 15-A). Spikes frequency decreased in both TBI groups as EEG recording progressed, with the frequency in the

CTBIHP group plateauing right away by the 4th week post-TBI (ranging between 16.845 ± 2.875 and 11.163 ± 0.494 spikes/hour), and gradually plateauing in the CTBINS group after 10 weeks post-TBI (ranging between 4.578 ± 0.31 and 6.078 ± 0.518 spikes/hour). At the end of the recording, 3 months post-TBI, the CTBIHP group still had a significantly higher frequency of spikes (11.71 ± 0.799 spikes/hour, $p < 0.05$) compared to the CTBINS group (5.725 ± 0.16 spikes/hour) (Figure 15-B).

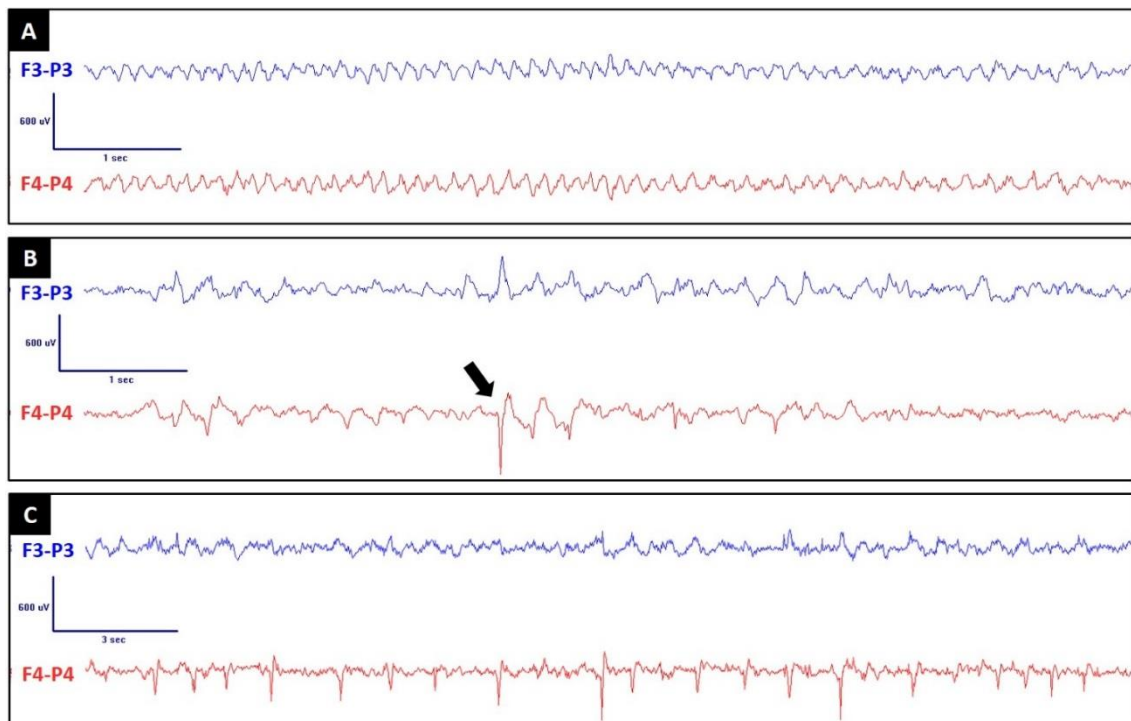


Figure 14. Spikes in TBI rats. Shown is the EEG tracing of one rat with 4 sampling electrodes (F3: left frontal, F4: right frontal, P3: left parietal, P4: right parietal), in the longitudinal bipolar montage where the blue line represents the left side of the brain (electrodes F3-P3) and the red line represent the right side of the brain (electrodes F4-P4) **Panel A:** baseline activity of 6 Hz, likely representing the thalamocortical-mediated posterior dominant rhythm, well described in humans. **Panel B:** shown is a single paroxysmal spike (black arrow) of 600 uV and < 250 ms duration. **Panel C:** multiple spikes with prominently higher amplitude in the right side of the brain, ipsilateral to the injury side.

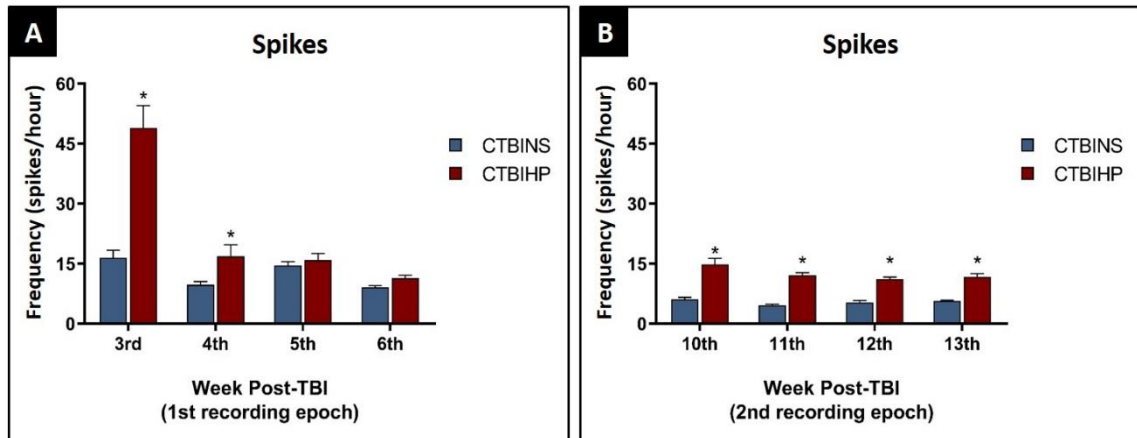


Figure 15. Quantification of spikes. Spikes were only detected in the TBI groups. **Panel A:** CTBIHP group had significantly more spikes per hour than the CTBINS group in the 3rd week post-TBI ($p < 0.05$, Two-Way ANOVA with post-hoc Fisher's LSD test). The number of spikes decreased in both groups over time. **Panel B:** Spikes persisted in both TBI groups and plateaued by the 13th week post-TBI (3 months), while remaining significantly higher in the heparinized CTBIHP group ($p < 0.05$, Two-Way ANOVA with post-hoc Fisher's LSD test). (NS= controls with normal saline $n=10$; HP= controls with heparin $n=8$; CTBINS= Closed-TBI with normal saline $n=14$; CTBIHP= Closed-TBI with heparin $n=11$). The results are reported as mean \pm SEM.

2. Polyspikes

Polyspikes (polyphasic spikes with two or more spike components) were detected in all groups (Figure 16). They may clinically manifest as wet-dog shakes in rodents. Polyspikes were detected in all groups. They were generalized and co-occurring in both hemispheres, but having a higher amplitude in the right hemisphere in the TBI groups (ipsilateral to the injury site). While polyspikes were detected in all rats, their frequency was substantially higher in TBI groups compared to both control groups ($p < 0.05$) (Figure 17-A). Furthermore, CTBIHP displayed a significantly higher number of polyspikes compared to CTBINS throughout the recording ($p < 0.05$). Polyspikes number decreased over time, and eventually plateaued, but remained significantly higher in the TBI groups, and more so in the heparinized CTBIHP group (Figure 17-B) (Ranges of polyspikes frequencies throughout EEG recording: NS: between 0.356 ± 0.089 and 1.2 ± 0.258 polyspikes/hour, HP: between 0.375 ± 0.072 0.943 and ± 0.124

polyspikes/hour, CTBINS: between 4.688 ± 0.879 and 19.777 ± 1.621 polyspikes/hour, CTBIHP: between 10.584 ± 0.41 and 30.297 ± 3.413 polyspikes/hour).

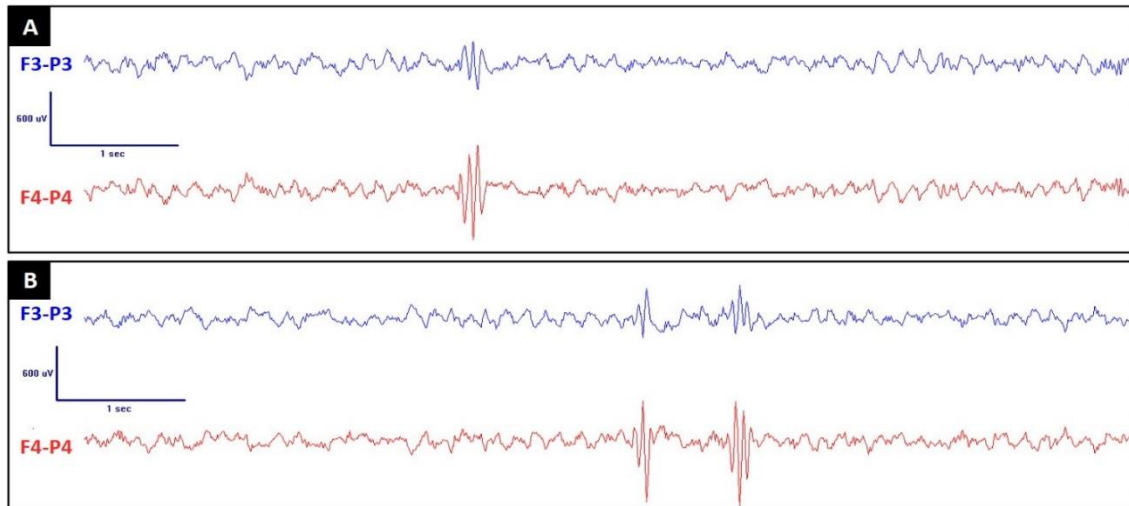


Figure 14. Polyspikes. Polyspikes were detected as polyphasic spikes with multiple spike components, that clearly disrupt the background electrical activity. They were observed on both hemispheres, having a higher amplitude in the right side of the brain in TBI groups. Polyspikes can appear as a single event (Panel A), or as consecutive events (Panel B).

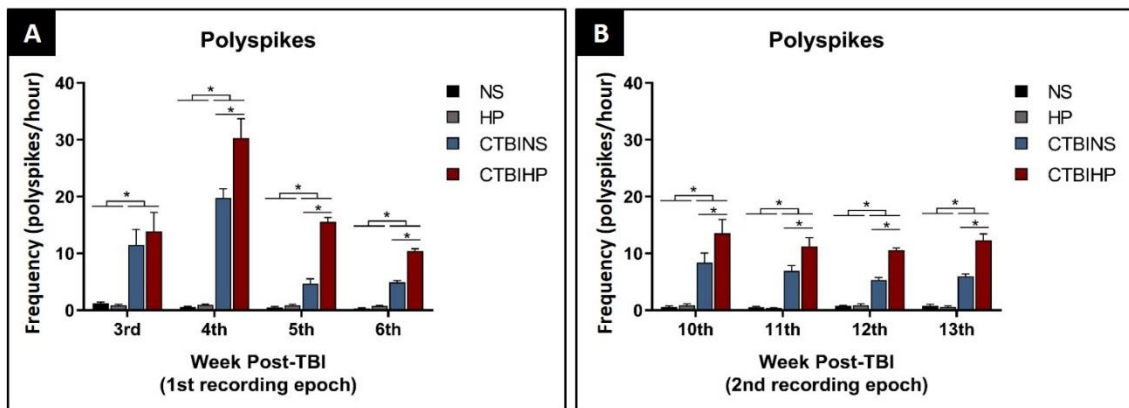


Figure 15. Quantification of polyspikes. Polyspikes were detected in all groups, but were significantly and consistently higher in the TBI groups compared to control groups ($p < 0.05$, Two-Way ANOVA with post-hoc Fisher's LSD test). The frequency of polyspikes decreased over time in both TBI groups (Panel A), and eventually plateaued. The CTBIHP group had a significantly higher frequency of polyspikes than the CTBINS group all throughout the recording ($p < 0.05$, Two-Way ANOVA with post-hoc Fisher's LSD test). (NS= controls with normal saline $n=10$; HP= controls with heparin $n=8$; CTBINS= Closed-TBI with normal saline $n=14$; CTBIHP= Closed-TBI with heparin $n=11$). The results are reported as mean \pm SEM.

C. MWM: visuospatial navigation

We investigated hippocampal-dependent visuospatial learning following hemorrhagic closed-head TBI using the Morris water maze. All rats gradually learned to reach the escape platform over the 5 training days (Figure 18-A) ($p < 0.05$, within-group comparison). However, on day 3 of training, Both TBI groups were significantly slower than their respective control groups in reaching the escape platform ($p < 0.05$). In the probe trial test, all groups showed comparable retention of spatial learning by spending significantly more time in the North-East (NE) quadrant (where the escape platform used to be) compared to the other quadrants ($p < 0.05$) (Figure 18-B). The escape latencies to the visible platform were comparable among all groups (Figure 18-C), suggesting no significant visual or locomotor deficits.

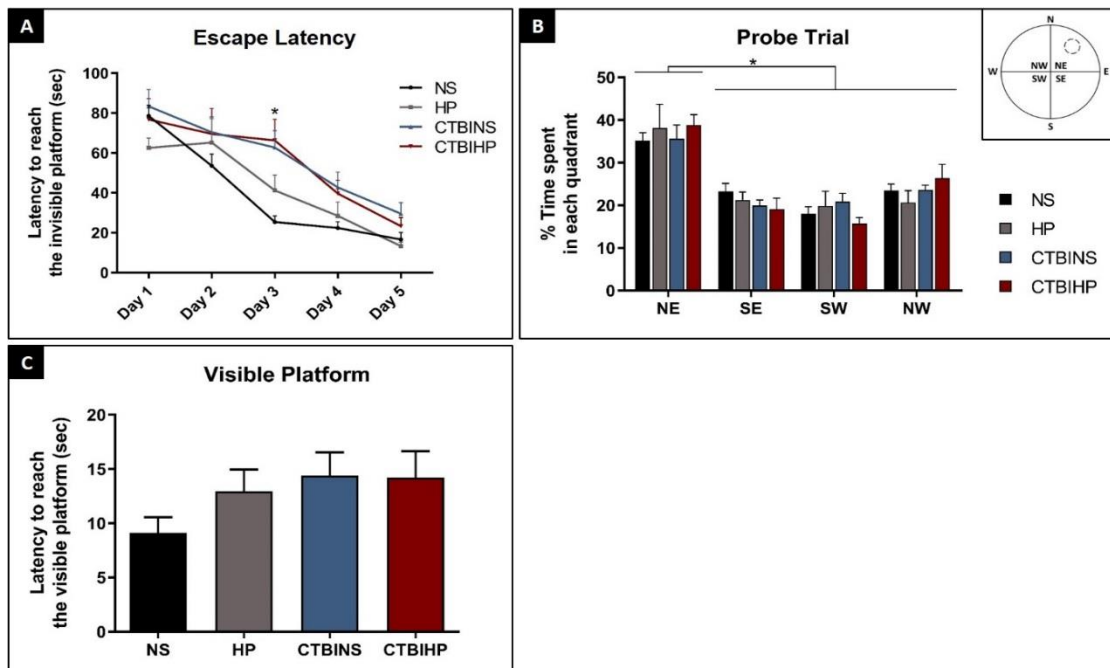


Figure 16. Visuospatial navigation in the Morris water maze. Panel A: escape latencies during the 5 acquisition days. All groups learned to reach the escape platform over the 5 training. However, on Day 3 both CTBIHP and CTBINS were significantly slower than both control groups ($p < 0.05$, Two-Way ANOVA with post-hoc Fisher's LSD test) (Escape latency on Day 3: NS= 25.389 ± 2.978 sec, HP= 40.178 ± 712 sec, CTBINS= 62.692 ± 8.44 sec, CTBIHP = 66.292 ± 10.574 sec). **Panel B:** the percentage of time spent in each of the four quadrants during the probe trial test. All groups significantly spent most of their time in the NE quadrant, where the invisible platform used to be ($p < 0.05$, ANOVA with post-hoc Fisher's LSD test). **Panel C:** escape latencies to the visible escape platform. All groups were comparable in reaching the visible platform ($p = 0.265$, One-Way ANOVA). (NE= North East; SE= South East; SW= South West; NW= North West) (NS= controls with normal saline $n=10$; HP= controls with heparin $n=8$; CTBINS= Closed-TBI with normal saline $n=14$; CTBIHP= Closed-TBI with heparin $n=11$). The results are reported as mean \pm SEM.

D. Rotarod: motor performance

The rotarod motor test was done as a complementary test to the Morris water maze to check for any motor deficits that could have affected the rats' swimming abilities. It was also performed to check if the injury considerably affected the motor cortex. All groups had comparable latencies to fall from the accelerating rotating rod ($p= 0.906$, One-Way ANOVA), suggesting comparable motor capabilities (Figure 19).

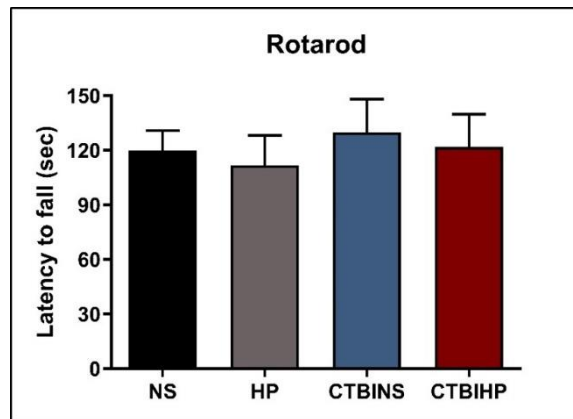


Figure 17. Rotarod performance. All groups had similar latencies to fall from the accelerating rotating rod ($p= 0.906$, One-Way ANOVA with post-hoc Fisher's LSD test). (NS: 119.9 ± 10.98 sec, HP: 111.8 ± 16.34 sec, CTBINS: 129.8 ± 18.24 sec, CTBIHP: 121.8 ± 17.99 sec). (NS= controls with normal saline $n=10$; HP= controls with heparin $n=8$; CTBINS= Closed-TBI with normal saline $n=14$; CTBIHP= Closed-TBI with heparin $n=11$). The results are reported as mean \pm SEM.

E. MAAV: recognition of auditory-signaled and context-cued shocks and acquisition of adaptive behavior

Amygdalohippocampal-dependent learning of emotional cues and adaptive shock-avoiding behaviors were investigated using the MAAV test. Over the 6 training days, all groups were comparable in learning to avoid the tone-signaled electrical foot-shocks in the left chamber ($p= 0.47$, Two-Way ANOVA) (Figure 20-A) and the context-cued electrical foot-shocks in the right chamber ($p= 0.95$, Two-Way ANOVA) (Figure 20-C). However, retention of contextual learning (Figure 20-D), was significantly lower

($p < 0.05$) in the CTBIHP ($36.3 \pm 13.83\%$) compared to its respective HP control group ($79.47 \pm 14.06\%$) and compared to the NS control group ($90.62 \pm 2\%$). The CTBINS ($55.35 \pm 11.79\%$) also exhibited a significant deficit in contextual retention when compared to its respective NS control group. Additionally, both TBI groups seem to have plateaued in their learning during the retention test of auditory learning (Figure 20-B).

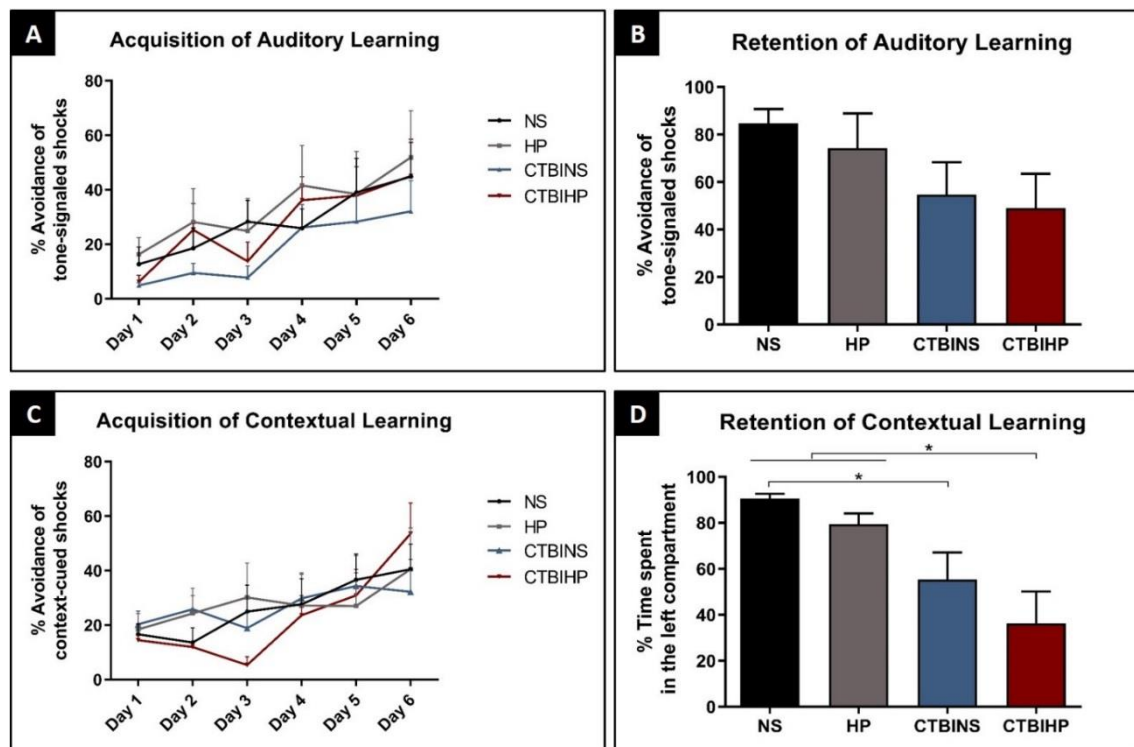


Figure 18. Avoidance of tone-sigaled (Panels A-B) and context-cued (Panels C-D) electrical foot-shocks. Panel A: acquisition of auditory learning. All groups had comparable learning curve of avoidance of tone-sigaled shocks during the 6 training days ($p = 0.47$, Two-Way ANOVA with post-hoc Fisher's LSD test). **Panel B:** all groups were comparable in retaining auditory learning (day 7). **Panel C:** acquisition of contextual learning. All groups had similar learning curves of avoidance of context-cued shocks. **Panel D:** retention of contextual learning on day 7. Contextual learning, assessed by measuring the time spent outside the right compartment, revealed retention deficits in both TBI groups ($p < 0.05$, One-Way ANOVA with post-hoc Fisher's LSD test) compared to their respective control groups (time spent in the "unthreatening" left compartment: NS= $90.26 \pm 2\%$, HP= $79.47 \pm 14.06\%$, CTBINS= $55.35 \pm 11.79\%$, CTBIHP= $36.29 \pm 13.83\%$). (NS= controls with normal saline $n=10$; HP= controls with heparin $n=8$; CTBINS= Closed-TBI with normal saline $n=11$; CTBIHP= Closed-TBI with heparin $n=14$). The results are reported as mean \pm SEM.

F. Von Frey and Hargreaves: sensory pathways integrity

The Von Frey and Hargreaves tests were done to assess for any sensory deficits that could be caused by the injury targeted over the parietal area (where the somatosensory cortex is found). They were also done as complements to the MAAV test to check for any deficits that could have affected the rats' ability to sense the electrical foot-shock. In the Von Frey filaments test (Figure 21-A), all groups had a comparable response rate to the mechanical stimuli in both hind paws ($p=0.89$). All rats had a higher response rate to the painful 15g filament compared to the unpainful 2g filament ($p<0.05$).

In the Hargreaves test (Figure 21-B), all groups had comparable withdrawal latency from the thermal stimulus in both hind paws ($p=0.465$).

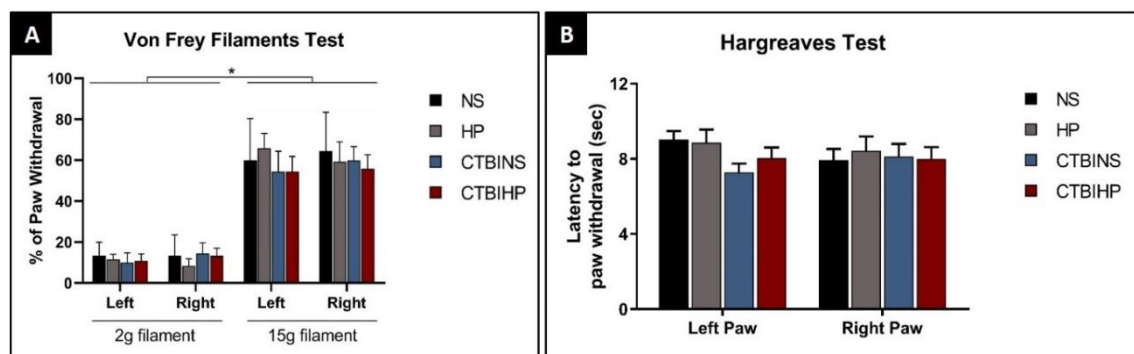


Figure 19. Paw withdrawal response to mechanical (Panel A) and thermal (Panel B) stimuli. Panel A: paw withdrawal response to non-painful (2g filament) and painful (15g filament) mechanical stimuli. All groups had comparable mechanical response in both hind paws ($p=0.89$, ANOVA with post-hoc Fisher's LSD test). Rats had higher response rate to the painful stimulus (15g filament) compared to the non-painful stimulus (2g filament) ($p<0.05$, ANOVA with post-hoc Fisher's LSD test). **Panel B:** paw withdrawal response to thermal stimulus. All groups had comparable withdrawal latency of both hind paws from the thermal stimulus ($p=0.465$, ANOVA with post-hoc Fisher's LSD test). (NS= controls with normal saline $n=10$; HP= controls with heparin $n=8$; CTBINS= Closed-TBI with normal saline $n=14$; CTBIHP= Closed-TBI with heparin $n=11$). The results are reported as mean \pm SEM.

G. Histological Analyses

We assessed reactive astrogliosis via GFAP immunostaining, 48 hours post-TBI (Figure 22) ($n=3$ in each group). In both the hippocampus and the parietal cortex, The

CTBIHP group showed significant astrogliosis marked by higher levels of GFAP compared to its respective control (HP group) and to the NS group ($p < 0.05$), while the CTBINS had similar levels compared to both controls. Notably, the CTBIHP group had a significantly higher level of GFAP compared to the CTBINS in the right hippocampus (ipsilateral to the injury site) ($p < 0.05$).

Cortical and hippocampal neuronal densities were assessed, 3 months post-TBI, by neuronal count of NeuN-positive cells (Figures 23). In both hippocampi, both TBI groups had significantly lower neuronal densities compared to their respective controls groups ($p < 0.05$). There was no statistical difference in neuronal densities in the parietal cortices between all groups ($p = 0.25$).

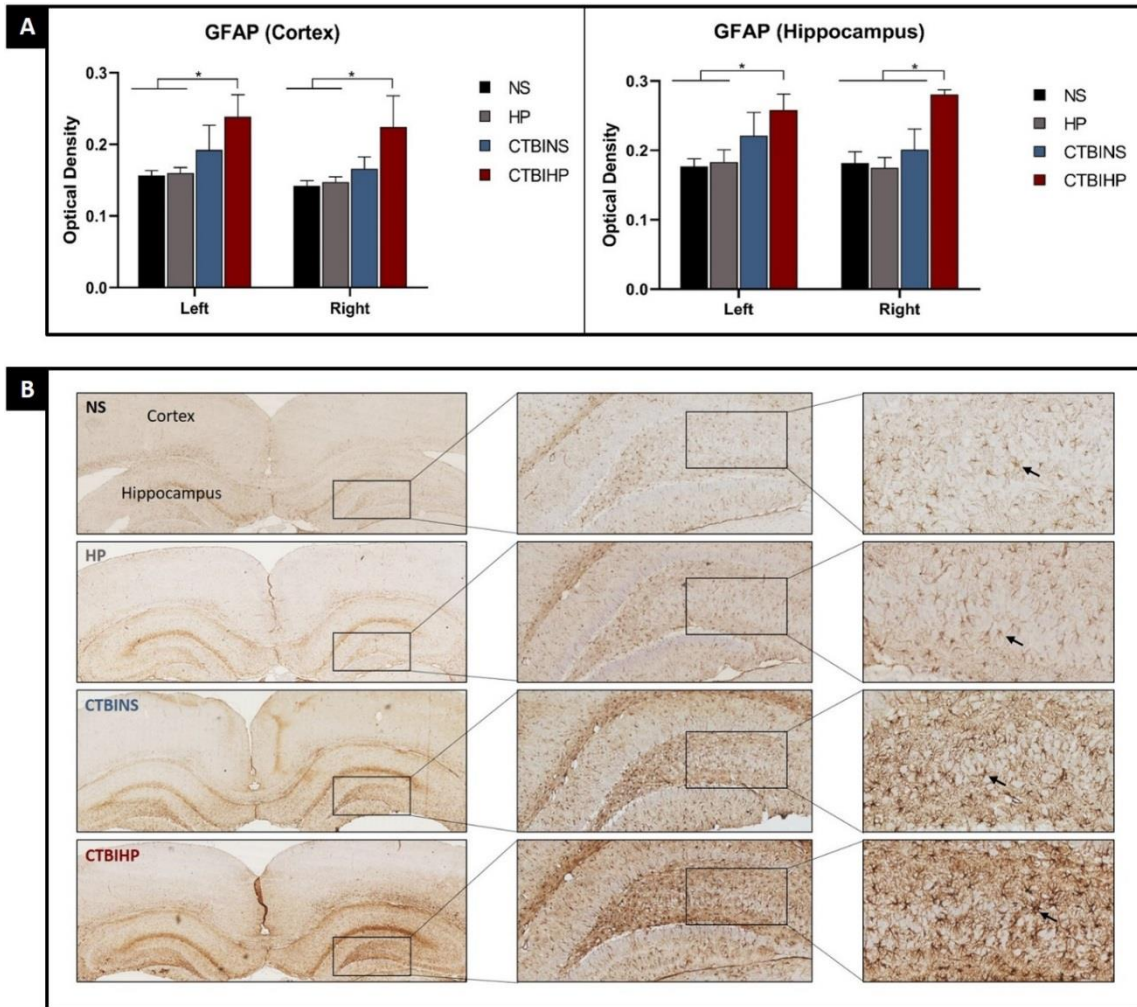


Figure 20. GFAP immunostaining. Panel A: Optical density of GFAP measured in the left and right parietal cortices and hippocampi. Compared to both control groups, the CTBIHP had a significant increase in the levels of GFAP in the parietal cortex and the hippocampus ($p < 0.05$, ANOVA with post-hoc Fisher's LSD). CTBIHP also had higher GFAP levels in the right hippocampus (ipsilateral to the injury side) compared to the CTBINS group ($p < 0.05$, ANOVA with post-hoc Fisher's LSD test). **Panel B:** representative images of GFAP staining. GFAP is a marker of "star-shaped" astrocytes (black arrows) and an increase in its levels is a hallmark of reactive astrogliosis. (NS= controls with normal saline $n=3$; HP= controls with heparin $n=3$; CTBINS= Closed-TBI with normal saline $n=3$; CTBIHP= Closed-TBI with heparin $n=3$). The results are reported as mean \pm SEM.

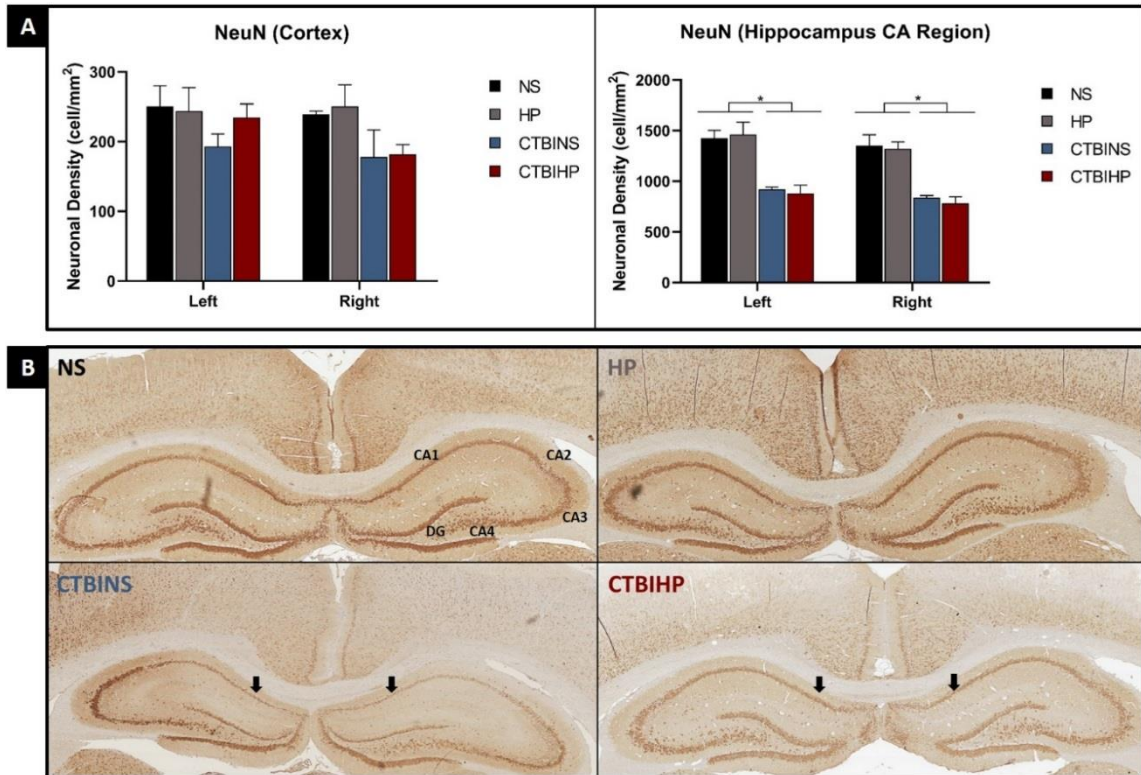


Figure 21. NeuN immunostaining. Panel A: Neuronal count in the left and right parietal cortices and hippocampi. Neuronal count in the CA1, CA2, and CA3 layers of the hippocampus revealed neuronal loss in both TBI groups compared to the controls ($p < 0.05$, ANOVA with post-hoc Fisher's LSD test) (Hippocampal neuronal density: NS= 1389.129 ± 93 cell/mm², HP= 1390.556 ± 95.5 cell/mm², CTBINS = 879 ± 23 , CTBIHP= 830 ± 75 cell/mm²). All groups had comparable neuronal density in the parietal cortex ($p = 0.25$, ANOVA with post-hoc Fisher's LSD test). **Panel B:** Representative images of NeuN staining, with a marked thinning of the CA1 layer in both TBI groups (black arrows). CA= cornu Ammonis; DG= dentate gyrus. (NS= controls with normal saline $n=3$; HP= controls with heparin $n=3$; CTBINS= Closed-TBI with normal saline $n=3$; CTBIHP= Closed-TBI with heparin $n=3$). The results are reported as mean \pm SEM.

CHAPTER V

DISCUSSION

Animal models are key platforms that allow researchers to explore potential novel therapies in controlled settings that are ethically and methodologically challenging in humans and not always safe. This is particularly true when facing the multiple complex mechanisms of epileptogenesis following TBI. Unfortunately, producing PTE in animal models faces many challenges, including high mortality rates, long latency period between TBI and PTE emergence, and the low percentage of rats that develop PTE, even in the most severe open-head models of TBI that are not as clinically-relevant as closed-head injuries [120, 128, 136, 137, 139, 141, 143, 148]. Indeed, closed-head injuries are far more common in humans, particularly in children, and PTE induced by closed-head TBI warrants more investigatory efforts. However, the rates of PTE are as low in rats as in humans, and when other researchers subjected EEG results to vigorous assessment, the PTE rates are even lower in rats (0-13%) [139, 141, 142, 147]. We hypothesized that the differences in the coagulation profile between rats and humans might be contributing to the low PTE rates in rats compared to humans, especially given the importance of hemorrhage as a risk factor for PTE [9, 108-110]. In this study, the use of an anti-coagulant successfully induced substantial hemorrhage consistently and reliably with no mortalities. In addition, heparinized TBI rats had a two-fold increase in the frequency of epileptiform features and a significant increase in hippocampal reactive astrogliosis, compared to the non-heparinized TBI rats, supporting the importance of excessive bleeding in hyperexcitability mechanisms following head injuries. Our outcomes suggest the development of a potentially permanent abnormal network of hyperexcitability (as discussed below), promoting the face validity of our

novel heparinized TBI model. The partial sacrifice of construct validity with the use of heparin improved the face validity of the electrographic and pathological outcomes. Our findings are also in line with the literature on seizure rodent models, where construct validity is often sacrificed with the use of chemicals in the most heavily employed models of acquired epilepsy (e.g., KA-model and pilocarpine model). These chemoconvulsants models accurately mimic the electrographic, pathological, and behavioral characteristics of human epilepsies, especially temporal lobe epilepsy, and thus, currently serve as the essential platforms to study novel anti-seizure strategies [155-159].

In this study, we reported an increase in TBI-induced epileptiform features with the promotion of substantial hemorrhage in heparinized TBI rats. While there is extensive literature on epileptiform and spikes discharges, there is an ongoing debate and controversy about the nature of spikes that are detected on the EEG following TBI in rodents, and whether they are epileptiform in nature. Some have argued that spikes that are found in controls are not epileptic; in other words, they do not reflect a TBI-induced epileptogenic network that results in seizure emergence [137, 142].

Occasionally, spikes in animals, as well as in humans, that are found in normal controls might be traits that appear on sleep transition, or age-dependent traits, or innate traits that worsen with brain insults [120, 142, 160, 161]. In order to avoid outcomes that may be clouded by discharges found in controls, we morphologically stratified the electrical discharges into spikes (a pointed spike with a repolarization wave, found primarily on the ipsilateral side of the injury) and polyspikes (a run of 2 or more spikes, found bilaterally). First, the electrical discharges that were found exclusively in TBI rats were

morphologically consistent with single spikes that are ipsilateral to the injury side (based on amplitude). These were interpreted as epileptiform and secondary to the TBI-induced hyperexcitability. When we reviewed the literature for studies that followed a similar methodology and found these discharges only in TBI rats, the rates ranged between 50% and 87% (depending on the model), as opposed to 100% rate of spike emergence in our TBI groups [139, 141, 143, 147]. One of these studies quantified these spikes and found an average of 11.5 spikes over the 2 weeks of EEG recording, which is less than our spikes frequency rates of 14 spikes/hour and 6 spikes/hour in the heparinized and non-heparinized TBI groups [143]. The persistence of these spikes up to three months post-TBI suggests the emergence of permanent abnormal brain circuitry and networks. Indeed, studies have reported that spikes might play an essential role in epileptogenesis by inducing and guiding axonal sprouting [96] and forming excitatory connections between neurons of the same network [97]. They may also have prognostic significance based on frequency correlation with seizure severity [162]. Various in vivo models show the crucial role of these post-traumatic spikes in the emergence of epileptogenesis. In the KA-model of temporal lobe epilepsy, spikes emerge before the provoked seizure, and the rate of development of epilepsy strongly correlates with the frequency and the cumulative number of EEG spikes after the initial brain insult [163], pointing to a higher risk of TBI-induced hyperexcitability with the promotion of hemorrhage and to a higher risk of seizures that may have emerged with longer recording period (ongoing work).

Second, in addition to spikes detection and quantification, the second morphological type of discharges were polyspikes. These were found in both sham-

manipulated controls and injured rats. However, polyspikes frequency substantially increased following TBI, and more so in the hemorrhagic group. Since they were found in controls, our polyspikes findings were interpreted as an increase of pre-existent excitability features following trauma, and more so when the trauma is coupled with hemorrhage promotion. This falls in line with our laboratory experience, whereby an increase of polyspikes, also found in controls, precedes seizure emergence in KA-injected rats, marking a worsening of hyperexcitability.

In this study, we reported pathological surrogates that may trace back the detected spikes to the hippocampus as the epileptogenic network. While we did not accurately localize the source of these epileptiform discharges with depth electrodes implanted in the hippocampi, we did detect histological changes consistent with a significant increase in GFAP levels, usually a hallmark of reactive astrogliosis that accompanies hippocampal epileptogenicity and seizures [164]. Interestingly, this increase in GFAP was only significantly found in the heparinized TBI group that had more prominent bleeding and epileptiform discharges. While astrogliosis is a widely described process in temporal lobe epilepsy in both humans and rodents [165-168], it is also specifically documented following TBI and particularly associated with PTE emergence [51, 134, 169]. This is attributed to the downregulation of homeostatic proteins, gap junctions, dysfunction and, impaired astrocytes coupling [134, 170, 171]. While seizures and epilepsy were thought to be exclusive *neuronal* diseases, an overwhelming amount of evidence suggest the crucial role of glial cells, including astrocytes, in epileptogenesis and seizure emergence mechanisms [134, 169, 171].

Moreover, here we assessed and quantified the levels of neuronal damage in both the cortex and the hippocampus, and found comparable neuronal loss in both TBI groups, that reached significance in the hippocampus but not in the cortex, probably due to the low number of sections per brain (ongoing work). However, hippocampal neuronal loss did not differ between the heparinized and the non-heparinized TBI groups, even though the frequency of epileptiform discharges was higher in the heparinized TBI group. Notably, there is a lack of correlation between the burden of hippocampal neuronal loss and the rate of emergence of hyperexcitable network and seizure and their severity. [172-174]. The formation of hyperexcitable networks may be due to synaptic reorganization, promoted by hemorrhage rather than by neuronal loss, especially given the susceptibility of the hippocampus to network reorganization and synaptic remodeling following TBI, particularly the CA1 and CA3 layers [84, 85], and the dentate gyrus that has been reported to sprout axonal collaterals into the inner molecular layer (i.e., mossy fiber sprouting).

Finally, in this study, we formed a neurobehavioral panel to assess sensorimotor and cognitive behavioral deficits. While the injury was targeted over the skull overlying the parietal area (somatosensory cortex), no sensory deficits were observed, and there were no frontal-related motor deficits, and therefore the results of the Morris water maze (MWM) and the modified active avoidance (MAAV) were attributed to hippocampus-related deficits in visuospatial navigation and contextual learning. In our novel MAAV test, TBI rats exhibited a significant deficit in the retention of contextual learning, but not in auditory learning, pointing to the MAAV sensitivity to the subtypes of instrumental conditioning. This behavioral profile suggests a milder hippocampal

injury that could only be detected in the MAAV. Indeed, detection of contextual learning deficits can sometimes be unidentifiable in the MWM, as evidenced by our experience in the hypoxic seizure model and the KA-model [175, 176].

In summary, closed-head injury with prominent hemorrhage produced potentially permanent abnormal networks of hyperexcitability, an essential landmark of epileptogenic mechanisms, paving the way for establishing a model with high rates of PTE emergence. In humans, the latency period between the injury time and the onset of PTE can be up to two years [68, 177], and this long latency period is also similarly found in rodents (months and up to a year) [135, 136, 139, 141, 143]. Due to time constraints, we obtained EEG recording for only 3 months, and it is possible that we have quantified epileptiform discharges during a period that represents the latency period. Spikes were detected in 100% of TBI rats, and their frequency was two-fold higher in the heparinized rats. While the presence of spikes does not necessarily destine all rats to become epileptic, rats with spikes have a higher risk of seizure emergence [119, 120, 128, 139, 143]. These electrographic changes were accompanied by evidence of hippocampal sclerosis in the heparinized TBI group, even if the risk of cognitive deficits was comparable with the non-heparinized group. These promising results will prompt us to engage in further investigations and extend the EEG recording period for more than 6 months post-TBI in order to detect the possible emergence of seizures in our herein described novel heparinized TBI model.

CHAPTER VI

LIMITATIONS AND FUTURE PERSPECTIVES

Post-traumatic epilepsy is a clinical condition with a long latency period in both humans and rodents that can span weeks to months across the board of this heterogeneous condition. This study had some limitations that can be traced back to time constraints, given the long-term nature of the sought outcomes. One of the main limitations of this study is, therefore, the lack of prolonged continuous EEG in order to detect potential late emergence of seizures in this herein described model. While unlikely, seizures might have occurred during the 3 weeks period of behavioral testing when EEG was interrupted. This calls the need for wireless EEG that allow continuous recording during the period of behavioral testing, and future studies aim to extend the EEG recording for more than 6 months. Besides, stereological analysis of histological results could have yielded a more accurate quantification of neuronal densities and GFAP levels, however, this was not done due to lack of software availability. The number of sections for IHC is being increased and additional outcome measures are being optimized, including acute injury markers (Fluor Jade) and neuroinflammation markers. Finally, we are aiming to establish the correlation between spikes frequency and the observed behavioral and histological results in individual rats, along with the characterization of the changes in sleep spindles, given that sleep disruption is a major TBI outcome.

REFERENCES

1. Xiong, Y., A. Mahmood, and M. Chopp, *Animal models of traumatic brain injury*. Nat Rev Neurosci, 2013. **14**(2): p. 128-42.
2. Strazzer, S., et al., *Late Post-traumatic Epilepsy in Children and Young Adults: Impropriety of Long-Term Antiepileptic Prophylaxis and Risks in Tapering*. Paediatr Drugs, 2016. **18**(3): p. 235-42.
3. Park, J.T. and H.T. Chugani, *Post-Traumatic Epilepsy in Children—Experience From a Tertiary Referral Center*. Pediatric Neurology, 2015. **52**(2): p. 174-181.
4. Appleton, R.E. and C. Demellweek, *Post-traumatic epilepsy in children requiring inpatient rehabilitation following head injury*. J Neurol Neurosurg Psychiatry, 2002. **72**(5): p. 669-72.
5. Taylor, C.A., et al., *Traumatic Brain Injury-Related Emergency Department Visits, Hospitalizations, and Deaths - United States, 2007 and 2013*. MMWR Surveill Summ, 2017. **66**(9): p. 1-16.
6. Parks, S., et al., *Characteristics of non-fatal abusive head trauma among children in the USA, 2003--2008: application of the CDC operational case definition to national hospital inpatient data*. Inj Prev, 2012. **18**(6): p. 392-8.
7. Halstead, M.E., et al., *Sport-Related Concussion in Children and Adolescents*. Pediatrics, 2018. **142**(6).
8. Narayan, R.K., et al., *Clinical trials in head injury*. J Neurotrauma, 2002. **19**(5): p. 503-57.
9. Siller-Matula, J.M., et al., *Interspecies differences in coagulation profile*. Thromb Haemost, 2008. **100**(3): p. 397-404.
10. Maxwell, W.L., *Damage to myelin and oligodendrocytes: a role in chronic outcomes following traumatic brain injury?* Brain Sci, 2013. **3**(3): p. 1374-94.
11. Injury, G.B.D.T.B. and C. Spinal Cord Injury, *Global, regional, and national burden of traumatic brain injury and spinal cord injury, 1990-2016: a systematic analysis for the Global Burden of Disease Study 2016*. Lancet Neurol, 2019. **18**(1): p. 56-87.
12. Dewan, M.C., et al., *Estimating the global incidence of traumatic brain injury*. J Neurosurg, 2018: p. 1-18.
13. Maas, A.I.R., et al., *Traumatic brain injury: integrated approaches to improve prevention, clinical care, and research*. Lancet Neurol, 2017. **16**(12): p. 987-1048.
14. Humphreys, I., et al., *The costs of traumatic brain injury: a literature review*. Clinicoecon Outcomes Res, 2013. **5**: p. 281-7.
15. Abou-Abbass, H., et al., *Epidemiology and clinical characteristics of traumatic brain injury in Lebanon: A systematic review*. Medicine (Baltimore), 2016. **95**(47): p. e5342.
16. Musharrafieh, U., et al., *Profile of injured patients presenting to a tertiary hospital in a developing country*. J Med Liban, 2011. **59**(4): p. 191-6.
17. Hwang, S.Y., et al., *Long-term outcomes in children with moderate to severe traumatic brain injury: a single-centre retrospective study*. Brain Inj, 2019. **33**(11): p. 1420-1424.
18. Hon, K.L., et al., *Mortality And Morbidity of Severe Traumatic Brain Injuries; A Pediatric Intensive Care Unit Experience Over 15 Years*. Bull Emerg Trauma, 2019. **7**(3): p. 256-262.
19. Aoki, M., et al., *Epidemiology, Patterns of treatment, and Mortality of Pediatric Trauma Patients in Japan*. Sci Rep, 2019. **9**(1): p. 917.
20. Jalalvandi, F., et al., *Epidemiology of Pediatric Trauma and Its Patterns in Western Iran: A Hospital Based Experience*. Glob J Health Sci, 2015. **8**(6): p. 139-46.

21. Keenan, H.T., et al., *Psychosocial and Executive Function Recovery Trajectories One Year after Pediatric Traumatic Brain Injury: The Influence of Age and Injury Severity*. J Neurotrauma, 2018. **35**(2): p. 286-296.
22. Keenan, H.T., et al., *Longitudinal Developmental Outcomes after Traumatic Brain Injury in Young Children: Are Infants More Vulnerable Than Toddlers?* J Neurotrauma, 2019. **36**(2): p. 282-292.
23. Anderson, V., et al., *Intellectual outcome from preschool traumatic brain injury: a 5-year prospective, longitudinal study*. Pediatrics, 2009. **124**(6): p. e1064-71.
24. Anderson, V., et al., *Predictors of cognitive function and recovery 10 years after traumatic brain injury in young children*. Pediatrics, 2012. **129**(2): p. e254-61.
25. Rivara, F.P., et al., *Disability 3, 12, and 24 months after traumatic brain injury among children and adolescents*. Pediatrics, 2011. **128**(5): p. e1129-38.
26. Bonnier, C., et al., *Neurodevelopmental outcome after severe traumatic brain injury in very young children: role for subcortical lesions*. J Child Neurol, 2007. **22**(5): p. 519-29.
27. Keenan, H.T., et al., *Neurodevelopmental consequences of early traumatic brain injury in 3-year-old children*. Pediatrics, 2007. **119**(3): p. e616-23.
28. Barlow, K.M., et al., *Late neurologic and cognitive sequelae of inflicted traumatic brain injury in infancy*. Pediatrics, 2005. **116**(2): p. e174-85.
29. Dewan, M.C., et al., *Epidemiology of Global Pediatric Traumatic Brain Injury: Qualitative Review*. World Neurosurg, 2016. **91**: p. 497-509 e1.
30. Maas, A.I.R., N. Stocchetti, and R. Bullock, *Moderate and severe traumatic brain injury in adults*. The Lancet Neurology, 2008. **7**(8): p. 728-741.
31. Vakil, M.T. and A.K. Singh, *A review of penetrating brain trauma: epidemiology, pathophysiology, imaging assessment, complications, and treatment*. Emerg Radiol, 2017. **24**(3): p. 301-309.
32. Mueller, K., et al., *Penetrating Brain Injury*. 2018. p. 420-444.e2.
33. Bales, J.W., R.H. Bonow, and R.G. Ellenbogen, *25 - Closed Head Injury*, in *Principles of Neurological Surgery (Fourth Edition)*, R.G. Ellenbogen, et al., Editors. 2018, Content Repository Only!: Philadelphia. p. 366-389.e4.
34. Martin, R.M., et al., *Traumatic hemorrhagic brain injury: impact of location and resorption on cognitive outcome*. J Neurosurg, 2017. **126**(3): p. 796-804.
35. Moen, K.G., et al., *Traumatic axonal injury: Relationships between lesions in the early phase and diffusion tensor imaging parameters in the chronic phase of traumatic brain injury*. J Neurosci Res, 2016. **94**(7): p. 623-35.
36. Jing, Z., et al., *Haemorrhagic shearing lesions associated with diffuse axonal injury: application of T2 star-weighted angiography sequence in the detection and clinical correlation*. Br J Neurosurg, 2011. **25**(5): p. 596-605.
37. Tong, K.A., et al., *Diffuse axonal injury in children: clinical correlation with hemorrhagic lesions*. Ann Neurol, 2004. **56**(1): p. 36-50.
38. Tong, K.A., et al., *Hemorrhagic shearing lesions in children and adolescents with posttraumatic diffuse axonal injury: improved detection and initial results*. Radiology, 2003. **227**(2): p. 332-9.
39. McKee, A.C. and D.H. Daneshvar, *The neuropathology of traumatic brain injury*. Handb Clin Neurol, 2015. **127**: p. 45-66.
40. Bryan, M.A., et al., *Sports- and Recreation-Related Concussions in US Youth*. Pediatrics, 2016. **138**(1).
41. Hunt, R.F., J.A. Boychuk, and B.N. Smith, *Neural circuit mechanisms of post-traumatic epilepsy*. Front Cell Neurosci, 2013. **7**: p. 89.

42. Andriessen, T.M., et al., *Epidemiology, severity classification, and outcome of moderate and severe traumatic brain injury: a prospective multicenter study*. J Neurotrauma, 2011. **28**(10): p. 2019-31.
43. Teasdale, G. and B. Jennett, *Assessment of coma and impaired consciousness. A practical scale*. Lancet, 1974. **2**(7872): p. 81-4.
44. Prince, C. and M.E. Bruhns, *Evaluation and Treatment of Mild Traumatic Brain Injury: The Role of Neuropsychology*. Brain Sci, 2017. **7**(8).
45. Yi, J.H. and A.S. Hazell, *Excitotoxic mechanisms and the role of astrocytic glutamate transporters in traumatic brain injury*. Neurochem Int, 2006. **48**(5): p. 394-403.
46. Andriessen, T.M., B. Jacobs, and P.E. Vos, *Clinical characteristics and pathophysiological mechanisms of focal and diffuse traumatic brain injury*. J Cell Mol Med, 2010. **14**(10): p. 2381-92.
47. Prins, M., et al., *The pathophysiology of traumatic brain injury at a glance*. Dis Model Mech, 2013. **6**(6): p. 1307-15.
48. Ertürk, A., et al., *Interfering with the Chronic Immune Response Rescues Chronic Degeneration After Traumatic Brain Injury*. The Journal of Neuroscience, 2016. **36**(38): p. 9962.
49. Simon, D.W., et al., *The far-reaching scope of neuroinflammation after traumatic brain injury*. Nature Reviews Neurology, 2017. **13**: p. 572.
50. Xiong, Y., A. Mahmood, and M. Chopp, *Current understanding of neuroinflammation after traumatic brain injury and cell-based therapeutic opportunities*. Chin J Traumatol, 2018. **21**(3): p. 137-151.
51. Burda, J.E., A.M. Bernstein, and M.V. Sofroniew, *Astrocyte roles in traumatic brain injury*. Exp Neurol, 2016. **275 Pt 3**: p. 305-315.
52. Pekny, M., et al., *Astrocytes: a central element in neurological diseases*. Acta Neuropathol, 2016. **131**(3): p. 323-45.
53. Johnson, V.E., et al., *Inflammation and white matter degeneration persist for years after a single traumatic brain injury*. Brain, 2013. **136**(Pt 1): p. 28-42.
54. Lipton, M.L., et al., *Multifocal white matter ultrastructural abnormalities in mild traumatic brain injury with cognitive disability: a voxel-wise analysis of diffusion tensor imaging*. J Neurotrauma, 2008. **25**(11): p. 1335-42.
55. Lipton, M.L., et al., *Diffusion-tensor imaging implicates prefrontal axonal injury in executive function impairment following very mild traumatic brain injury*. Radiology, 2009. **252**(3): p. 816-24.
56. Rosenfeld, J.V., et al., *Early management of severe traumatic brain injury*. The Lancet, 2012. **380**(9847): p. 1088-1098.
57. Scaratti, C., et al., *Work-related difficulties in patients with traumatic brain injury: a systematic review on predictors and associated factors*. Disabil Rehabil, 2017. **39**(9): p. 847-855.
58. Cruz-Haces, M., et al., *Pathological correlations between traumatic brain injury and chronic neurodegenerative diseases*. Transl Neurodegener, 2017. **6**: p. 20.
59. *Neuropsychiatric Assessment*, in *Textbook of Traumatic Brain Injury*.
60. Albrecht, J.S., et al., *Risk of Depression after Traumatic Brain Injury in a Large National Sample*. J Neurotrauma, 2019. **36**(2): p. 300-307.
61. Emery, C.A., et al., *A Systematic Review of Psychiatric, Psychological, and Behavioural Outcomes following Mild Traumatic Brain Injury in Children and Adolescents*. Can J Psychiatry, 2016. **61**(5): p. 259-69.
62. Perry, D.C., et al., *Association of traumatic brain injury with subsequent neurological and psychiatric disease: a meta-analysis*. J Neurosurg, 2016. **124**(2): p. 511-26.

63. *Neurocognitive Disorders*, in *Textbook of Traumatic Brain Injury*. 2018, American Psychiatric Association Publishing.
64. Rao, V., et al., *Neuropsychiatric disturbances associated with traumatic brain injury: a practical approach to evaluation and management*. *Semin Neurol*, 2015. **35**(1): p. 64-82.
65. Narad, M.E., et al., *Secondary Attention-Deficit/Hyperactivity Disorder in Children and Adolescents 5 to 10 Years After Traumatic Brain Injury*. *JAMA Pediatrics*, 2018. **172**(5): p. 437.
66. Pitkanen, A. and R. Immonen, *Epilepsy related to traumatic brain injury*. *Neurotherapeutics*, 2014. **11**(2): p. 286-96.
67. Frey, L.C., *Epidemiology of posttraumatic epilepsy: a critical review*. *Epilepsia*, 2003. **44**(s10): p. 11-7.
68. Englander, J., et al., *Analyzing risk factors for late posttraumatic seizures: a prospective, multicenter investigation*. *Arch Phys Med Rehabil*, 2003. **84**(3): p. 365-73.
69. Lowenstein, D.H., *Epilepsy after head injury: an overview*. *Epilepsia*, 2009. **50** Suppl 2: p. 4-9.
70. Fisher, R.S., et al., *Epileptic seizures and epilepsy: definitions proposed by the International League Against Epilepsy (ILAE) and the International Bureau for Epilepsy (IBE)*. *Epilepsia*, 2005. **46**(4): p. 470-2.
71. Stafstrom, C.E. and L. Carmant, *Seizures and epilepsy: an overview for neuroscientists*. Cold Spring Harb Perspect Med, 2015. **5**(6).
72. Wilson, J.V. and E.H. Reynolds, *Texts and documents. Translation and analysis of a cuneiform text forming part of a Babylonian treatise on epilepsy*. *Med Hist*, 1990. **34**(2): p. 185-98.
73. Magiorkinis, E., K. Sidiropoulou, and A. Diamantis, *Hallmarks in the history of epilepsy: epilepsy in antiquity*. *Epilepsy Behav*, 2010. **17**(1): p. 103-8.
74. Panteliadis, C.P., et al., *Historical documents on epilepsy: From antiquity through the 20th century*. *Brain Dev*, 2017. **39**(6): p. 457-463.
75. Thomas, S.V. and A. Nair, *Confronting the stigma of epilepsy*. *Annals of Indian Academy of Neurology*, 2011. **14**(3): p. 158-163.
76. Brodie, M., *The history and stigma of epilepsy*. supplement, *Epilepsia*, 2003. **44**: p. 12-14.
77. Collaborators, G.B.D.E., *Global, regional, and national burden of epilepsy, 1990-2016: a systematic analysis for the Global Burden of Disease Study 2016*. *Lancet Neurol*, 2019. **18**(4): p. 357-375.
78. Fisher, R.S., et al., *Operational classification of seizure types by the International League Against Epilepsy: Position Paper of the ILAE Commission for Classification and Terminology*. *Epilepsia*, 2017. **58**(4): p. 522-530.
79. Somboon, T., M.M. Grigg-Damberger, and N. Foldvary-Schaefer, *Epilepsy and Sleep-Related Breathing Disturbances*. *Chest*, 2019. **156**(1): p. 172-181.
80. Kandel, E.R., et al., *Principles of neural science*. Vol. 4. 2000: McGraw-hill New York.
81. Pitkanen, A., et al., *Epileptogenesis*. Cold Spring Harb Perspect Med, 2015. **5**(10).
82. Ben-Ari, Y., *Excitatory actions of gaba during development: the nature of the nurture*. *Nat Rev Neurosci*, 2002. **3**(9): p. 728-39.
83. Jirsa, V.K., et al., *On the nature of seizure dynamics*. *Brain*, 2014. **137**(Pt 8): p. 2210-30.
84. Scheff, S.W., et al., *Synaptogenesis in the hippocampal CA1 field following traumatic brain injury*. *J Neurotrauma*, 2005. **22**(7): p. 719-32.
85. Norris, C.M. and S.W. Scheff, *Recovery of afferent function and synaptic strength in hippocampal CA1 following traumatic brain injury*. *J Neurotrauma*, 2009. **26**(12): p. 2269-78.

86. Dudek, F.E. and K.J. Staley, *The time course of acquired epilepsy: implications for therapeutic intervention to suppress epileptogenesis*. *Neurosci Lett*, 2011. **497**(3): p. 240-6.
87. Sloviter, R.S., *Permanently altered hippocampal structure, excitability, and inhibition after experimental status epilepticus in the rat: the "dormant basket cell" hypothesis and its possible relevance to temporal lobe epilepsy*. *Hippocampus*, 1991. **1**(1): p. 41-66.
88. Sloviter, R.S., et al., *"Dormant basket cell" hypothesis revisited: relative vulnerabilities of dentate gyrus mossy cells and inhibitory interneurons after hippocampal status epilepticus in the rat*. *J Comp Neurol*, 2003. **459**(1): p. 44-76.
89. Sun, C., et al., *Selective loss of dentate hilar interneurons contributes to reduced synaptic inhibition of granule cells in an electrical stimulation-based animal model of temporal lobe epilepsy*. *J Comp Neurol*, 2007. **500**(5): p. 876-93.
90. Zhang, W. and P.S. Buckmaster, *Dysfunction of the dentate basket cell circuit in a rat model of temporal lobe epilepsy*. *J Neurosci*, 2009. **29**(24): p. 7846-56.
91. Gupta, A., et al., *Decrease in tonic inhibition contributes to increase in dentate semilunar granule cell excitability after brain injury*. *J Neurosci*, 2012. **32**(7): p. 2523-37.
92. Raible, D.J., et al., *GABA(A) receptor regulation after experimental traumatic brain injury*. *J Neurotrauma*, 2012. **29**(16): p. 2548-54.
93. Marcuse, L.V., M.C. Fields, and J. Yoo, *4 - The abnormal EEG*, in *Rowan's Primer of EEG (Second Edition)*, L.V. Marcuse, M.C. Fields, and J. Yoo, Editors. 2016, Elsevier: London. p. 87-119.
94. Staley, K.J., A. White, and F.E. Dudek, *Interictal spikes: harbingers or causes of epilepsy?* *Neurosci Lett*, 2011. **497**(3): p. 247-50.
95. Tao, J.X., et al., *Cortical substrates of scalp EEG epileptiform discharges*. *J Clin Neurophysiol*, 2007. **24**(2): p. 96-100.
96. Carmichael, S.T. and M.F. Chesselet, *Synchronous neuronal activity is a signal for axonal sprouting after cortical lesions in the adult*. *J Neurosci*, 2002. **22**(14): p. 6062-70.
97. Staley, K., J.L. Hellier, and F.E. Dudek, *Do interictal spikes drive epileptogenesis?* *Neuroscientist*, 2005. **11**(4): p. 272-6.
98. Stafstrom, C.E., *Interictal spikes: memories forsaken*. *Epilepsy Curr*, 2010. **10**(5): p. 135-6.
99. Binnie, C.D., *Cognitive impairment during epileptiform discharges: is it ever justifiable to treat the EEG?* *Lancet Neurol*, 2003. **2**(12): p. 725-30.
100. Kleen, J.K., et al., *Hippocampal interictal epileptiform activity disrupts cognition in humans*. *Neurology*, 2013. **81**(1): p. 18-24.
101. Danielsson, J. and F. Petermann, *Cognitive deficits in children with benign rolandic epilepsy of childhood or rolandic discharges: a study of children between 4 and 7 years of age with and without seizures compared with healthy controls*. *Epilepsy Behav*, 2009. **16**(4): p. 646-51.
102. Fonseca, L.C., G.M. Tedrus, and E.M. Pacheco, *Epileptiform EEG discharges in benign childhood epilepsy with centrotemporal spikes: reactivity and transitory cognitive impairment*. *Epilepsy Behav*, 2007. **11**(1): p. 65-70.
103. Fonseca, L.C., et al., *Benign childhood epilepsy with centro-temporal spikes: correlation between clinical, cognitive and EEG aspects*. *Arq Neuropsiquiatr*, 2007. **65**(3A): p. 569-75.
104. Rosati, A., et al., *Intractable temporal lobe epilepsy with rare spikes is less severe than with frequent spikes*. *Neurology*, 2003. **60**: p. 1290-1295.
105. Krendl, R., S. Lurger, and C. Baumgartner, *Absolute spike frequency predicts surgical outcome in TLE with unilateral hippocampal atrophy*. *Neurology*, 2008. **71**(6): p. 413-8.

106. Cascino, G.D., et al., *Long-term follow-up of stereotactic lesionectomy in partial epilepsy: predictive factors and electroencephalographic results*. *Epilepsia*, 1992. **33**(4): p. 639-44.
107. *Clinical Imaging*, in *Textbook of Traumatic Brain Injury*, T. McAllister and D.B. Arciniegas, Editors.
108. Liesemer, K., et al., *Early post-traumatic seizures in moderate to severe pediatric traumatic brain injury: rates, risk factors, and clinical features*. *J Neurotrauma*, 2011. **28**(5): p. 755-62.
109. Ritter, A.C., et al., *Incidence and risk factors of posttraumatic seizures following traumatic brain injury: A Traumatic Brain Injury Model Systems Study*. *Epilepsia*, 2016. **57**(12): p. 1968-1977.
110. Kim, J.A., et al., *Epileptiform activity in traumatic brain injury predicts post-traumatic epilepsy*. *Ann Neurol*, 2018. **83**(4): p. 858-862.
111. Angeleri, F., et al., *Posttraumatic epilepsy risk factors: one-year prospective study after head injury*. *Epilepsia*, 1999. **40**(9): p. 1222-30.
112. Messori, A., et al., *Predicting posttraumatic epilepsy with MRI: prospective longitudinal morphologic study in adults*. *Epilepsia*, 2005. **46**(9): p. 1472-81.
113. Willmore, L.J., *Post-traumatic epilepsy: cellular mechanisms and implications for treatment*. *Epilepsia*, 1990. **31 Suppl 3**: p. S67-73.
114. Willmore, L.J. and Y. Ueda, *Posttraumatic epilepsy: hemorrhage, free radicals and the molecular regulation of glutamate*. *Neurochem Res*, 2009. **34**(4): p. 688-97.
115. Mahler, B., et al., *Unprovoked seizures after traumatic brain injury: A population-based case-control study*. *Epilepsia*, 2015. **56**(9): p. 1438-44.
116. Tubi, M.A., et al., *Early seizures and temporal lobe trauma predict post-traumatic epilepsy: A longitudinal study*. *Neurobiol Dis*, 2018.
117. Chen, W., et al., *Risk of post-traumatic epilepsy after severe head injury in patients with at least one seizure*. *Neuropsychiatr Dis Treat*, 2017. **13**: p. 2301-2306.
118. Haltiner, A.M., N.R. Temkin, and S.S. Dikmen, *Risk of seizure recurrence after the first late posttraumatic seizure*. *Arch Phys Med Rehabil*, 1997. **78**(8): p. 835-40.
119. Bragin, A., et al., *Pathologic electrographic changes after experimental traumatic brain injury*. *Epilepsia*, 2016. **57**(5): p. 735-45.
120. Reid, A.Y., et al., *The progression of electrophysiologic abnormalities during epileptogenesis after experimental traumatic brain injury*. *Epilepsia*, 2016. **57**(10): p. 1558-1567.
121. Lucke-Wold, B.P., et al., *Traumatic brain injury and epilepsy: Underlying mechanisms leading to seizure*. *Seizure*, 2015. **33**: p. 13-23.
122. Yeh, C.C., et al., *Risk of epilepsy after traumatic brain injury: a retrospective population-based cohort study*. *J Neurol Neurosurg Psychiatry*, 2013. **84**(4): p. 441-5.
123. Dixon, C.E., et al., *A fluid percussion model of experimental brain injury in the rat*. *J Neurosurg*, 1987. **67**(1): p. 110-9.
124. McIntosh, T.K., et al., *Traumatic brain injury in the rat: characterization of a lateral fluid-percussion model*. *Neuroscience*, 1989. **28**(1): p. 233-44.
125. Graham, D.I., et al., *Recent advances in neurotrauma*. *J Neuropathol Exp Neurol*, 2000. **59**(8): p. 641-51.
126. Hamm, R.J., *Neurobehavioral assessment of outcome following traumatic brain injury in rats: an evaluation of selected measures*. *J Neurotrauma*, 2001. **18**(11): p. 1207-16.
127. Morales, D.M., et al., *Experimental models of traumatic brain injury: do we really need to build a better mousetrap?* *Neuroscience*, 2005. **136**(4): p. 971-89.
128. Kharatishvili, I., et al., *A model of posttraumatic epilepsy induced by lateral fluid-percussion brain injury in rats*. *Neuroscience*, 2006. **140**(2): p. 685-97.
129. Cernak, I., *Animal models of head trauma*. *NeuroRx*, 2005. **2**(3): p. 410-22.

130. Cole, J.T., et al., *Craniotomy: true sham for traumatic brain injury, or a sham of a sham?* J Neurotrauma, 2011. **28**(3): p. 359-69.
131. Floyd, C.L., et al., *Craniectomy position affects morris water maze performance and hippocampal cell loss after parasagittal fluid percussion.* J Neurotrauma, 2002. **19**(3): p. 303-16.
132. Vink, R., et al., *Small shifts in craniotomy position in the lateral fluid percussion injury model are associated with differential lesion development.* J Neurotrauma, 2001. **18**(8): p. 839-47.
133. Lighthall, J.W., *Controlled cortical impact: a new experimental brain injury model.* J Neurotrauma, 1988. **5**(1): p. 1-15.
134. Shandra, O., et al., *Repetitive Diffuse Mild Traumatic Brain Injury Causes an Atypical Astrocyte Response and Spontaneous Recurrent Seizures.* J Neurosci, 2019. **39**(10): p. 1944-1963.
135. Bugay, V., et al., *A mouse model of repetitive blast traumatic brain injury reveals post-trauma seizures and increased neuronal excitability.* J Neurotrauma, 2019.
136. Kelly, K.M., et al., *Posttraumatic seizures and epilepsy in adult rats after controlled cortical impact.* Epilepsy Res, 2015. **117**: p. 104-16.
137. Smith, D., et al., *Convulsive seizures and EEG spikes after lateral fluid-percussion injury in the rat.* Epilepsy Res, 2018. **147**: p. 87-94.
138. Guo, D., et al., *Rapamycin attenuates the development of posttraumatic epilepsy in a mouse model of traumatic brain injury.* PLoS One, 2013. **8**(5): p. e64078.
139. Bolkvadze, T. and A. Pitkanen, *Development of post-traumatic epilepsy after controlled cortical impact and lateral fluid-percussion-induced brain injury in the mouse.* J Neurotrauma, 2012. **29**(5): p. 789-812.
140. Hunt, R.F., S.W. Scheff, and B.N. Smith, *Posttraumatic epilepsy after controlled cortical impact injury in mice.* Exp Neurol, 2009. **215**(2): p. 243-52.
141. Statler, K.D., et al., *A potential model of pediatric posttraumatic epilepsy.* Epilepsy Res, 2009. **86**(2-3): p. 221-3.
142. Rodgers, K.M., F.E. Dudek, and D.S. Barth, *Progressive, Seizure-Like, Spike-Wave Discharges Are Common in Both Injured and Uninjured Sprague-Dawley Rats: Implications for the Fluid Percussion Injury Model of Post-Traumatic Epilepsy.* J Neurosci, 2015. **35**(24): p. 9194-204.
143. Shultz, S.R., et al., *Can structural or functional changes following traumatic brain injury in the rat predict epileptic outcome?* Epilepsia, 2013. **54**(7): p. 1240-50.
144. D'Ambrosio, R., et al., *Post-traumatic epilepsy following fluid percussion injury in the rat.* Brain, 2004. **127**(Pt 2): p. 304-14.
145. D'Ambrosio, R., et al., *Functional definition of seizure provides new insight into post-traumatic epileptogenesis.* Brain, 2009. **132**(10): p. 2805-2821.
146. Curia, G., et al., *Impact of injury location and severity on posttraumatic epilepsy in the rat: role of frontal neocortex.* Cereb Cortex, 2011. **21**(7): p. 1574-92.
147. Kharatishvili, I., et al., *Quantitative diffusion MRI of hippocampus as a surrogate marker for post-traumatic epileptogenesis.* Brain, 2007. **130**(Pt 12): p. 3155-68.
148. Kendirli, M.T., D.T. Rose, and E.H. Bertram, *A model of posttraumatic epilepsy after penetrating brain injuries: effect of lesion size and metal fragments.* Epilepsia, 2014. **55**(12): p. 1969-77.
149. Hara, T., et al., *Species differences in anticoagulant and anti-Xa activity of DX-9065a, a highly selective factor Xa inhibitor.* Thromb Res, 1995. **80**(1): p. 99-104.
150. Willner, P., *The validity of animal models of depression.* Psychopharmacology (Berl), 1984. **83**(1): p. 1-16.

151. Medlej, Y., et al., *Enhanced setup for wired continuous long-term EEG monitoring in juvenile and adult rats: application for epilepsy and other disorders*. BMC Neurosci, 2019. **20**(1): p. 8.
152. Medlej, Y., et al., *Methods in Electrode Implantation and Wiring for Long-Term Continuous EEG Monitoring in Rodent Models of Epilepsy and Behavioral Disturbances*. Methods Mol Biol, 2019. **2011**: p. 429-439.
153. Salah, H., et al., *Methods in Emotional Behavioral Testing in Immature Epilepsy Rodent Models*. Methods Mol Biol, 2019. **2011**: p. 413-427.
154. Medlej, Y., et al., *Overview on Emotional Behavioral Testing in Rodent Models of Pediatric Epilepsy*. Methods Mol Biol, 2019. **2011**: p. 345-367.
155. Minjarez, B., et al., *Behavioral changes in models of chemoconvulsant-induced epilepsy: A review*. Neurosci Biobehav Rev, 2017. **83**: p. 373-380.
156. Levesque, M., M. Avoli, and C. Bernard, *Animal models of temporal lobe epilepsy following systemic chemoconvulsant administration*. J Neurosci Methods, 2016. **260**: p. 45-52.
157. Levesque, M. and M. Avoli, *The kainic acid model of temporal lobe epilepsy*. Neurosci Biobehav Rev, 2013. **37**(10 Pt 2): p. 2887-99.
158. Curia, G., et al., *The pilocarpine model of temporal lobe epilepsy*. J Neurosci Methods, 2008. **172**(2): p. 143-57.
159. Loscher, W., *Animal Models of Seizures and Epilepsy: Past, Present, and Future Role for the Discovery of Antiseizure Drugs*. Neurochem Res, 2017. **42**(7): p. 1873-1888.
160. Britton, J.W., et al., *Electroencephalography (EEG): An introductory text and atlas of normal and abnormal findings in adults, children, and infants*. 2016: American Epilepsy Society, Chicago.
161. Pearce, P.S., et al., *Spike-wave discharges in adult Sprague-Dawley rats and their implications for animal models of temporal lobe epilepsy*. Epilepsy & Behavior, 2014. **32**: p. 121-131.
162. Yardi, R., et al., *Interictal Spikes on Intracranial EEG as a Potential Biomarker of Epilepsy Severity (P4.071)*. Neurology, 2016. **86**.
163. White, A., et al., *EEG spike activity precedes epilepsy after kainate-induced status epilepticus*. Epilepsia, 2010. **51**(3): p. 371-83.
164. Sofroniew, M.V., *Astrogliosis*. Cold Spring Harb Perspect Biol, 2014. **7**(2): p. a020420.
165. Iyengar, S., *Reactive Astrogliosis in Epilepsy-Passive Bystanders no more*. J Neurol Stroke, 2016. **5**(4): p. 00186.
166. Vargas-Sanchez, K., et al., *Astroglial role in the pathophysiology of status epilepticus: an overview*. Oncotarget, 2018. **9**(42): p. 26954-26976.
167. Fedele, D.E., et al., *Astrogliosis in epilepsy leads to overexpression of adenosine kinase, resulting in seizure aggravation*. Brain, 2005. **128**(Pt 10): p. 2383-95.
168. Devinsky, O., et al., *Glia and epilepsy: excitability and inflammation*. Trends Neurosci, 2013. **36**(3): p. 174-84.
169. Robel, S., et al., *Reactive astrogliosis causes the development of spontaneous seizures*. J Neurosci, 2015. **35**(8): p. 3330-45.
170. Wetherington, J., G. Serrano, and R. Dingledine, *Astrocytes in the epileptic brain*. Neuron, 2008. **58**(2): p. 168-78.
171. Robel, S. and H. Sontheimer, *Glia as drivers of abnormal neuronal activity*. Nat Neurosci, 2016. **19**(1): p. 28-33.
172. Obeid, M., et al., *Neuroprotective effects of leptin following kainic acid-induced status epilepticus*. Epilepsy Behav, 2010. **19**(3): p. 278-83.
173. Dudek, F.E., J.J. Ekstrand, and K.J. Staley, *Is neuronal death necessary for acquired epileptogenesis in the immature brain?* Epilepsy Curr, 2010. **10**(4): p. 95-9.

174. Dingledine, R., N.H. Varvel, and F.E. Dudek, *When and how do seizures kill neurons, and is cell death relevant to epileptogenesis?* Adv Exp Med Biol, 2014. **813**: p. 109-22.
175. Medlej, Y., et al., *Lestaurtinib (CEP-701) modulates the effects of early life hypoxic seizures on cognitive and emotional behaviors in immature rats.* Epilepsy Behav, 2019. **92**: p. 332-340.
176. Mikati, M.A., et al., *Long-term effects of acute and of chronic hypoxia on behavior and on hippocampal histology in the developing brain.* Brain Res Dev Brain Res, 2005. **157**(1): p. 98-102.
177. Cotter, D., A. Kelso, and A. Neligan, *Genetic biomarkers of posttraumatic epilepsy: A systematic review.* Seizure, 2017. **46**: p. 53-58.